the mixed culture. We therefore examined the basal expression levels of astrocyte L-Glu transporters and the effect of LPS on their expression levels. To compare the expression levels of GLAST and GLT1, we first compared the densities of western blotting bands for the same amount of GLAST and GLT1 control proteins (full length) (1, 10 μg) obtained at the same appropriate exposure time (Figure B, upper photos). Then, we quantified the expression levels of GLAST and GLT1 in the control- and LPS-treated mixed culture (Figure B, middle photos). The density of each band obtained at the same appropriate exposure time was normalized to the 10 μg control band of the corresponding subtype. Basally, the GLAST protein level is much higher than that of GLT1 (Figure 2, graph). The GLAST protein levels decreased to 65.7 ± 7.40% of control levels after LPS treatment (10 ng/mL, 72 h) (Figure 2C), but the GLT-1 protein level did not change. These results suggest that the LPS-induced increase in the L-Glu remaining was mainly caused by the downregulation of GLAST.

Activated microglia caused the decrease in L-Glu uptake during inflammation without cell death

To confirm that activated microglia are essential for the decrease in L-Glu uptake during inflammation without cell death, we examined the effects of LPS in four different types of cultures, including an astrocyte-microglia-neuron mixed culture (a), an astrocyte culture (b), an astrocyte-microglia co-culture (c), and an astrocyte-neuron co-culture (d) (Figure 3A). In (a), the astrocytes were confluent, and the cell densities of the microglia and the neurons were 3.0×10^4 cells/cm^2 and 6.0×10^4 cells/cm^2, respectively. Therefore, the cell density of the microglia in (c) and that of neurons in (d) were carefully adjusted to 3.0×10^4 cells/cm^2 and 6.0×10^4 cells/cm^2, respectively. Furthermore, in (b) to (d), we confirmed that the density of each cell type that had been presumably removed was sufficiently low; the number of microglia in (b) and (d) was $<1.2 \times 10^3$ cells/cm^2, and the number of neurons in (b) and (c) was $<1.0 \times 10^3$ cells/cm^2. Astrocytes

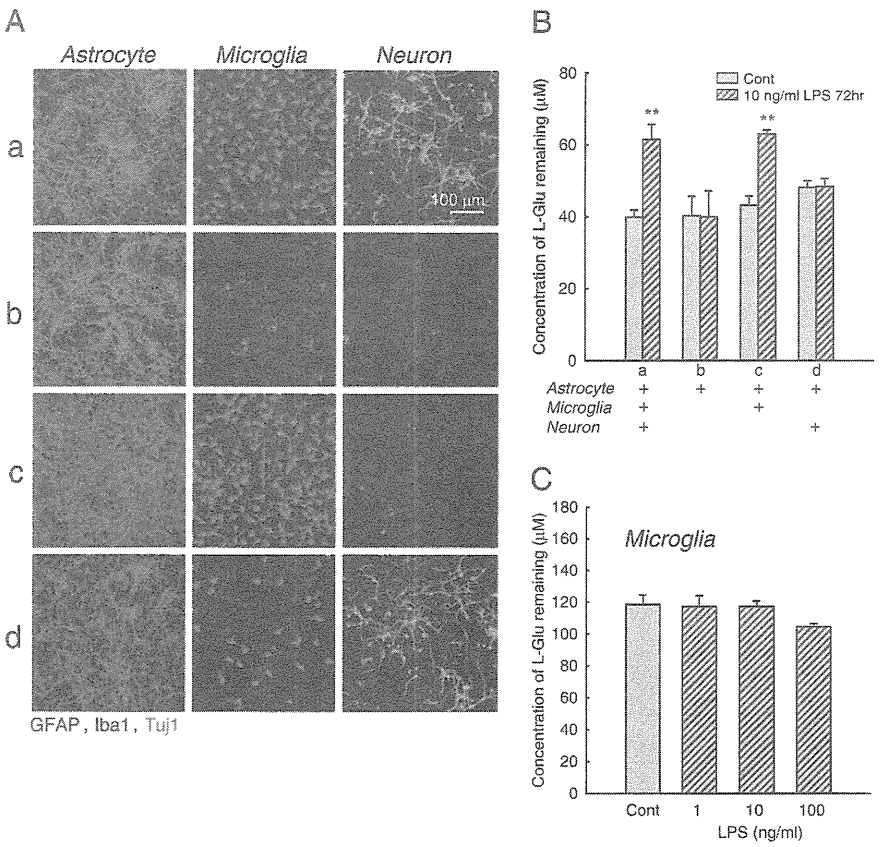

Figure 3 Activated microglia are essential for the decrease in L-Glu uptake in the model of inflammation without cell death. (**A**) Immunostaining of four types of cultures: astrocyte-microglia-neuron mixed culture (a), astrocyte culture (b), astrocyte-microglia co-culture (c), and neuron-astrocyte co-culture (d). (**B**) The effects of LPS (10 ng/mL, 72 h) on the concentration of L-Glu remaining in the four types of culture. Inhibitory effects were obtained in (a) and (c). $^{**}P < 0.01$ *vs.* control group ($n = 6$), Student's *t*-test. (**C**) The effects of LPS (10 ng/mL, 72 h) on the concentration of L-Glu remaining in microglial pure culture. The concentration of L-Glu remaining did not change during the assay (30 min).

were confluent in (a) to (d). When we treated these cultures with LPS (10 ng/mL, 72 h), significant decreases in L-Glu uptake occurred in (a) and (c) but not in (b) nor (d). As shown in Figure 3B (b), the L-Glu uptake in astrocyte pure culture was not changed by LPS. We further confirmed that in the LPS-treated microglial pure culture, the concentration of L-Glu remaining did not change during the assay (30 min) (Figure 3C). These results indicate that the increase in L-Glu remaining, that is, the inhibition of L-Glu uptake, observed in Figure 3B (a) and (c) was caused by the interaction between the activated microglia and the astrocytes during 72 h of LPS treatment.

L-Glu released from activated microglia caused the downregulation of GLAST expression during inflammation without cell death

Activated microglia release various soluble factors in inflammatory processes [16,18-24]. To examine the involvement of these factors in the action of activated microglia on L-Glu transporters, we applied the

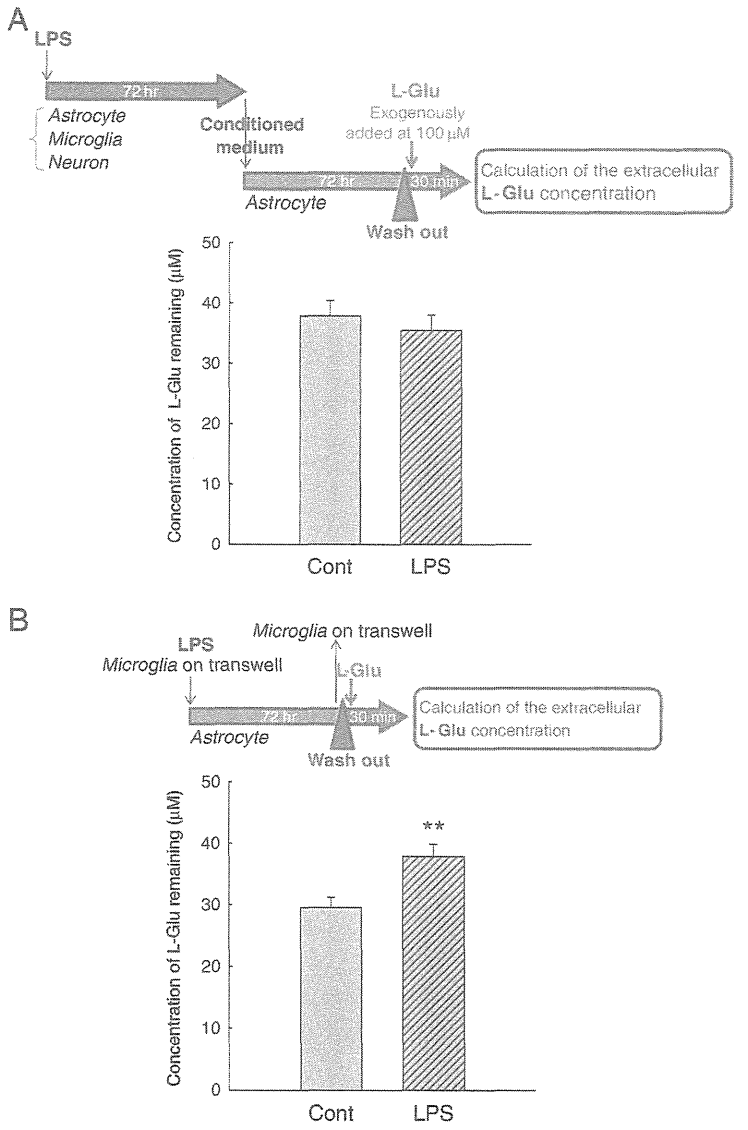

Figure 4 Transwell carrying activated microglia, but not the conditioned medium, decreased L-Glu uptake in the astrocyte culture. (**A**) Effect of the conditioned medium collected from the astrocyte-microglia-neuron mixed culture treated with LPS (10 ng/mL, 72 h) on L-Glu clearance in the astrocyte culture. A 72-h incubation with the conditioned medium did not affect L-Glu clearance in the astrocyte culture. (**B**) The effects of transwell-cultured microglia in the presence of LPS (10 ng/mL, 72 h) on L-Glu uptake in the astrocyte culture. A significant decrease in the L-Glu uptake was caused by 72-h treatment with the transwell. $^{**}P < 0.01$ *vs.* control group ($n = 6$), Student's *t*-test.

conditioned medium collected from the inflammation without cell death model (Figure 4A) to a culture of astrocytes alone. A 72 h-incubation with the conditioned medium did not affect the L-Glu uptake in the astrocyte culture. We then incubated the astrocyte culture with a transwell on which microglia were cultured in the presence of LPS (10 ng/mL, 72 h) (Figure 4B). Notably, a significant decrease in L-Glu uptake was obtained under these conditions. Because LPS in this condition did not directly affect the L-Glu uptake in the astrocyte culture, as shown in Figure 3B (b), these results suggest that the secreted factors are released from microglia and are degraded or taken up after their release. ATP has been shown to downregulate GLAST through the P2X7 receptor [28] and the ectonucleotidases of astrocytes rapidly convert extracellular ATP to ADP, ultimately to AMP [34]. We first examined the contribution of ATP to the downregulation of GLAST in the inflammation model without cell death. Exogenous application of ATP (Figure 5A) and P2X7 agonist BzATP (Figure 5B) did not change the L-Glu uptake. We also confirmed that neither the P2X receptor antagonist TNP-ATP (Figure 5C) nor the P2X7-specific antagonist BBG (Figure 5D) inhibited the decrease in L-Glu uptake in this inflammation model. We then examined the possibility of L-Glu. L-Glu is released by activated microglia through hemichannels [21,22] and taken up by L-Glu transporters after its release. We hypothesized that the secreted factor may be L-Glu. We first examined whether L-Glu was indeed released from microglia during inflammation without cell death. As shown in Figure 6A, left, LPS elevated the extracellular L-Glu concentrations in the astrocyte-microglia-neuron mixed cultures, and a significant elevation was observed even at a concentration of 1 ng/mL (Figure 6A left). An elevation of the extracellular L-Glu concentration was observed in

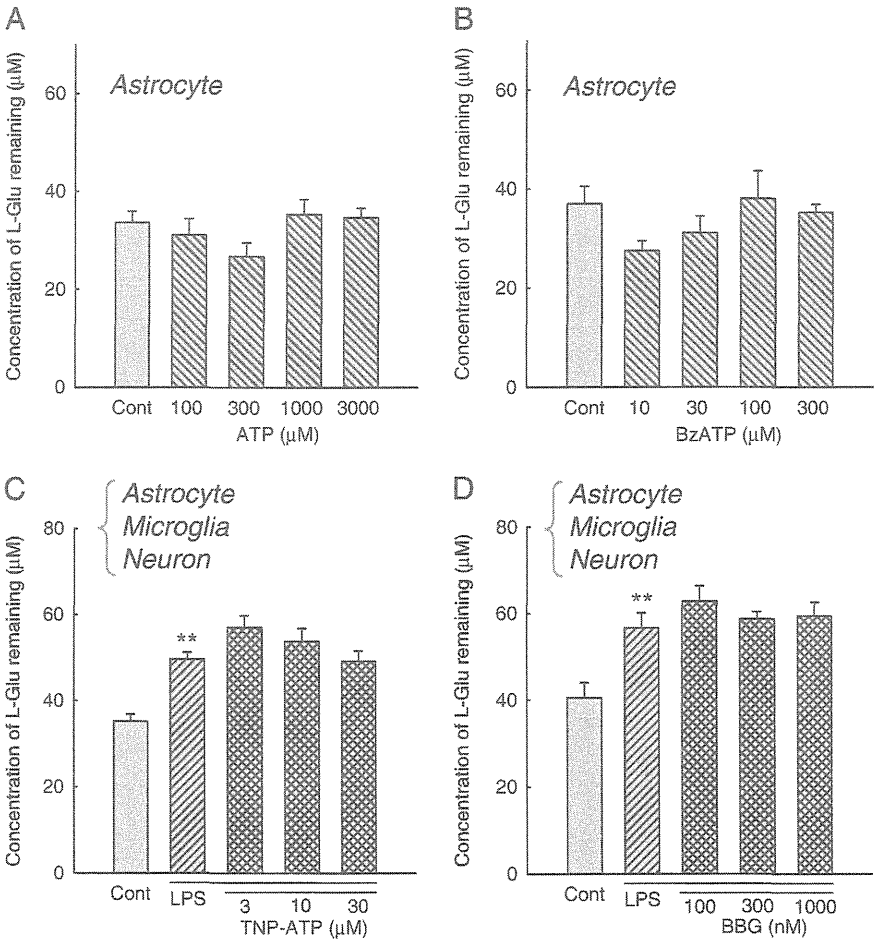

Figure 5 ATP did not contribute to the downregulation of GLAST in the inflammation without cell death. (**A**, **B**) Neither ATP nor the P2X7 agonist BzATP affected L-Glu uptake. (**C**, **D**) Neither the P2X receptor antagonist TNP-ATP nor the P2X7 specific antagonist BBG affected the LPS-induced decrease in L-Glu uptake. $^{**}P < 0.01$ *vs.* control group ($n = 6$), Tukey's test following ANOVA.

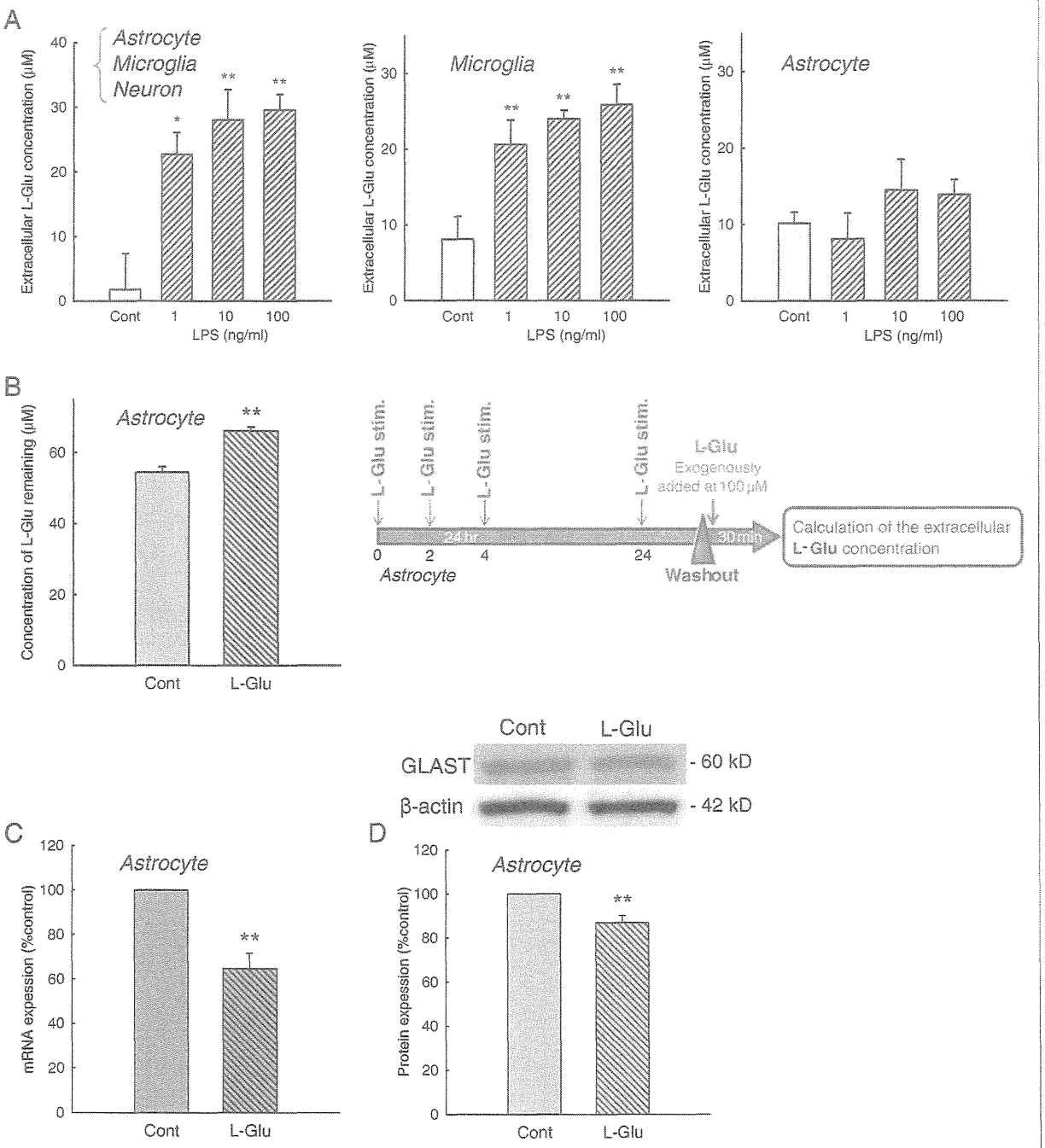

Figure 6 L-Glu released from activated microglia caused the downregulation of GLAST. (**A**) Effects of LPS (1 to 100 ng/mL, 24 h) on the extracellular concentration of L-Glu in the astrocyte-microglia-neuron mixed culture (left), microglia culture (center), and astrocyte culture (right). LPS significantly increased the extracellular L-Glu in the astrocyte-microglia-neuron mixed culture and the microglia culture. $^{*}P < 0.05$, $^{**}P < 0.01$ *vs.* control group ($n = 6$), Tukey's test following ANOVA. (**B**) The effect of sustained exposure to L-Glu on L-Glu clearance in the astrocyte culture. The culture medium was changed to fresh medium containing 100 μM L-Glu every 2 h. L-Glu clearance was suppressed by sustained exposure to L-Glu for 24 h. $^{**}P < 0.01$ *vs.* the control group ($n = 6$), Student's *t*-test. (**C**) The effect of sustained exposure to L-Glu on GLAST mRNA levels. Sustained exposure to L-Glu decreased GLAST mRNA. $^{**}P < 0.01$ *vs.* control group ($n = 4$), Student's *t*-test. (**D**) The effect of sustained exposure to L-Glu on GLAST protein levels. Sustained exposure to L-Glu decreased the protein expression of GLAST. $^{**}P < 0.01$ *vs.* control group ($n = 5$), Student's *t*-test.

the microglia culture (Figure 6A center) but not in the astrocyte culture (Figure 6A right). These results indicate that L-Glu was released from activated microglia during inflammation without cell death. To confirm our hypothesis, we tested the effect of the sustained elevation of extracellular L-Glu on L-Glu uptake in the mixed culture. To yield a sustained elevation of extracellular L-Glu, the culture medium of the astrocyte culture was freshly supplemented with 100 μM L-Glu every 2 h for 24 h, as preliminary studies showed that a concentration of 100 μM extracellular L-Glu was reduced to almost zero after 4 h in confluent astrocyte cultures (not shown). As shown in Figure 6B, the sustained elevation of extracellular L-Glu resulted in a significant decrease in L-Glu uptake in the astrocyte culture. GLAST expression was significantly decreased at the mRNA level

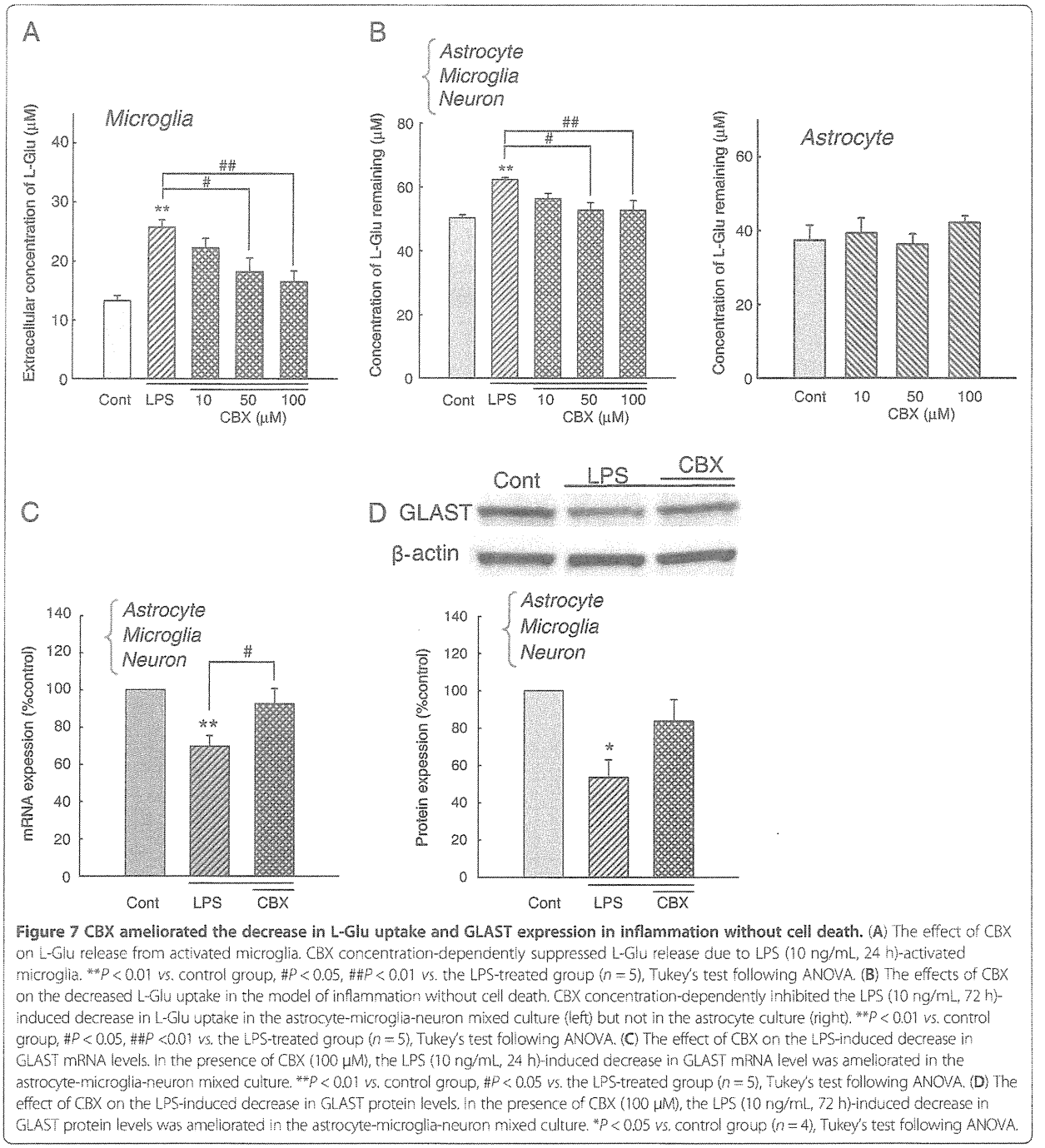

Figure 7 CBX ameliorated the decrease in L-Glu uptake and GLAST expression in inflammation without cell death. (**A**) The effect of CBX on L-Glu release from activated microglia. CBX concentration-dependently suppressed L-Glu release due to LPS (10 ng/mL, 24 h)-activated microglia. $^{**}P < 0.01$ *vs.* control group, $^{\#}P < 0.05$, $^{\#\#}P < 0.01$ *vs.* the LPS-treated group ($n = 5$), Tukey's test following ANOVA. (**B**) The effects of CBX on the decreased L-Glu uptake in the model of inflammation without cell death. CBX concentration-dependently inhibited the LPS (10 ng/mL, 72 h)-induced decrease in L-Glu uptake in the astrocyte-microglia-neuron mixed culture (left) but not in the astrocyte culture (right). $^{**}P < 0.01$ *vs.* control group, $^{\#}P < 0.05$, $^{\#\#}P < 0.01$ *vs.* the LPS-treated group ($n = 5$), Tukey's test following ANOVA. (**C**) The effect of CBX on the LPS-induced decrease in GLAST mRNA levels. In the presence of CBX (100 μM), the LPS (10 ng/mL, 24 h)-induced decrease in GLAST mRNA level was ameliorated in the astrocyte-microglia-neuron mixed culture. $^{**}P < 0.01$ *vs.* control group, $^{\#}P < 0.05$ *vs.* the LPS-treated group ($n = 5$), Tukey's test following ANOVA. (**D**) The effect of CBX on the LPS-induced decrease in GLAST protein levels. In the presence of CBX (100 μM), the LPS (10 ng/mL, 72 h)-induced decrease in GLAST protein levels was ameliorated in the astrocyte-microglia-neuron mixed culture. $^{*}P < 0.05$ *vs.* control group ($n = 4$), Tukey's test following ANOVA.

(Figure 6C) and the protein level (Figure 6D) by the same treatment. These results suggest that L-Glu was responsible for the decrease in L-Glu uptake during inflammation without cell death. When the microglia cultures were treated with LPS (10 ng/mL, 24 h) in the absence or presence of the hemichannel inhibitor, CBX (10 to 100 μM), the L-Glu release from the activated microglia was suppressed in a concentration-dependent manner (Figure 7A). CBX (100 μM) almost completely prevented the LPS-induced (10 ng/mL, 72 h) decrease in L-Glu uptake in the mixed culture (Figure 7B, left) but had no effect in the astrocyte culture (Figure 7B, right). Furthermore, CBX reversed the LPS-induced downregulation of GLAST expression at the mRNA (Figure 7C) and protein levels (Figure 7D).

We next tried to clarify the mechanisms through which the sustained elevation of extracellular L-Glu downregulates GLAST. Recent reports have suggested that the expression of L-Glu transporters is regulated by L-Glu through metabotropic glutamate receptors (mGluRs). We therefore first examined the involvement of metabotropic glutamate receptors (mGluRs). Neither the group I mGluR agonist DHPG nor the group II mGluR agonist DCG-4 affected either L-Glu uptake

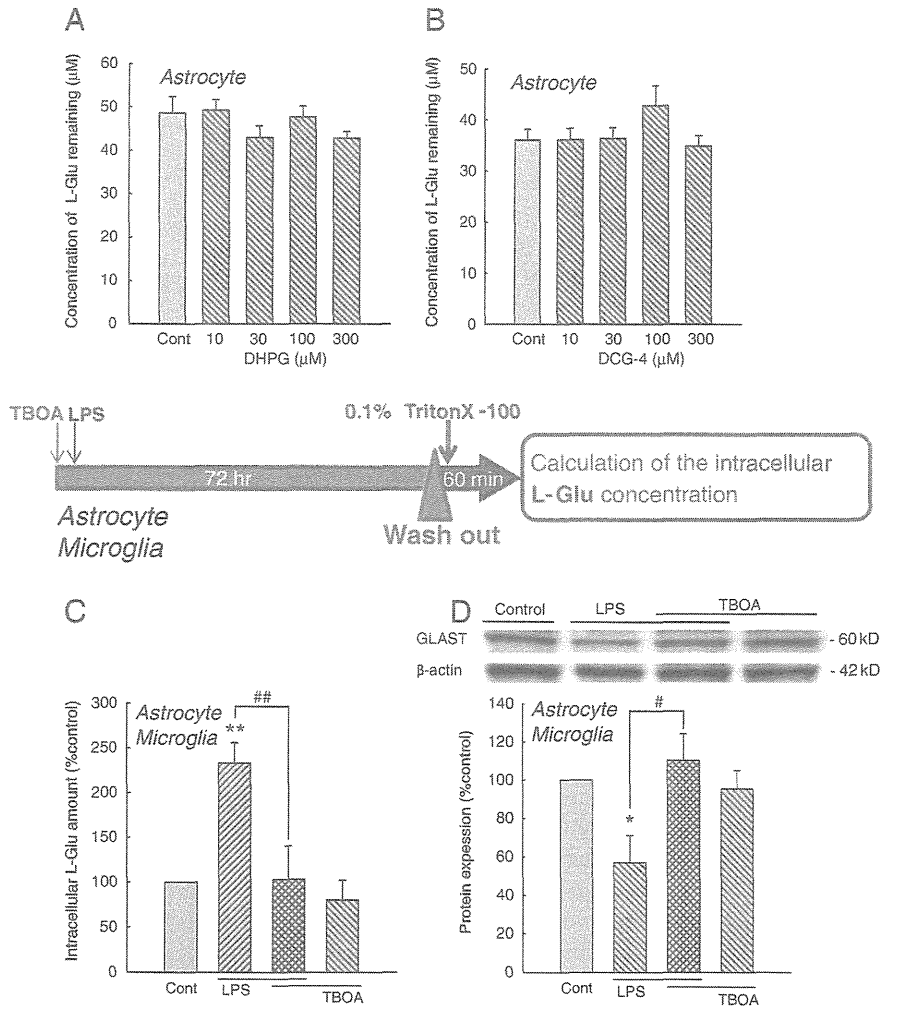

Figure 8 The elevation of intracellular L-Glu in astrocytes is important for the downregulation of GLAST. (**A**, **B**) The effects of mGluR agonists on L-Glu uptake. Neither the group I mGluR agonist DHPG (A) nor the group II mGluR agonist DCG-4 (B) affected L-Glu uptake. (**C**) The amount of astrocytic intracellular L-Glu after LPS-treatment in the absence or presence of TBOA in astrocyte-microglia co-cultures. LPS significantly increased the amount of astrocytic intracellular L-Glu, and TBOA completely suppressed this increase. $^{**}P < 0.01$ *vs.* control group, $^{\#\#}P < 0.01$ *vs.* the LPS-treated group ($n = 6$), Tukey's test following ANOVA. (**D**) The astrocytic expression of GLAST after LPS treatment in the absence or presence of TBOA in astrocyte-microglia co-cultures. TBOA suppressed the downregulation GLAST caused by LPS. $^{*}P < 0.05$ *vs.* control group, $^{\#}P < 0.05$ *vs.* the LPS-treated group ($n = 6$), Tukey's test following ANOVA.

(Figure 8A and B) or the expression level of GLAST (not shown). Sustained elevation of extracellular L-Glu caused by activated microglia is expected to cause the elevation of intracellular L-Glu in astrocytes. We therefore examined whether the elevation of intracellular L-Glu itself is important for the downregulation of GLAST. To do this, we first measured the amount of astrocytic intracellular L-Glu after LPS-treatment in the absence or presence of TBOA in astrocyte-microglia co-cultures (Figure 8C). LPS significantly increased the amount of intracellular L-Glu, and TBOA completely suppressed this increase. Western blotting showed that TBOA suppressed the downregulation GLAST caused by LPS (Figure 8D). TBOA itself did not have effects on either the amount of intracellular L-Glu or the GLAST protein level. These results indicate that the elevation of astrocytic intracellular L-Glu, but not the signaling cascade from the cell surface, is important for the downregulation of GLAST.

Our findings suggest that activated microglia trigger the elevation of extracellular L-Glu through their own release of L-Glu, astrocyte L-Glu transporters are downregulated by the elevation of astrocytic intracellular L-Glu, and further elevation of extracellular L-Glu occurs early in neuroinflammation. A schematic model of this 'collusion' hypothesis is shown in Figure 9.

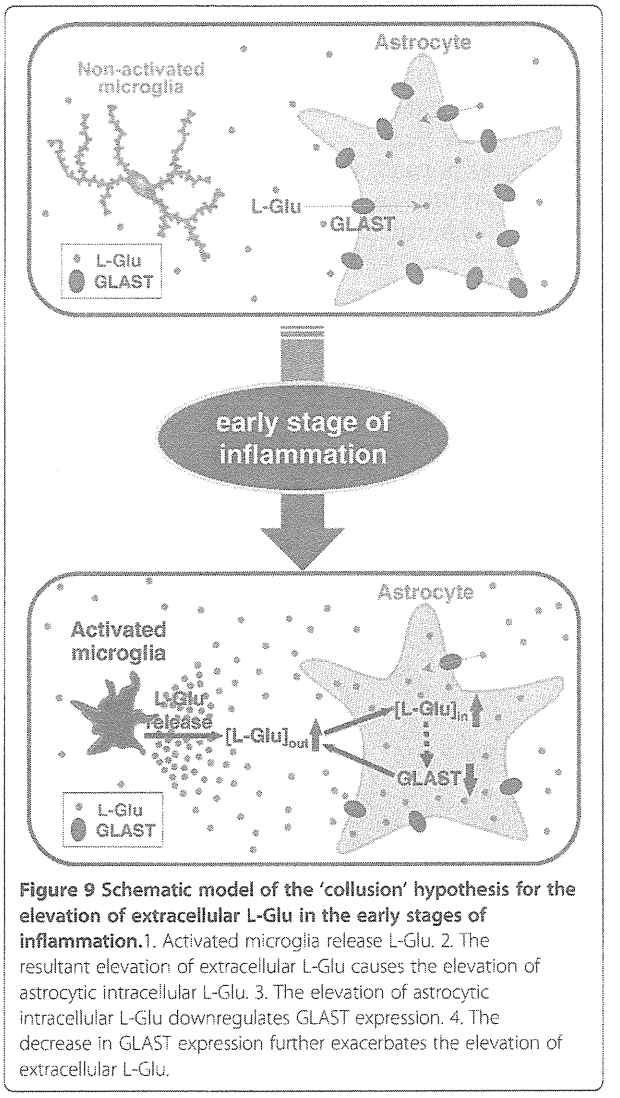

Figure 9 Schematic model of the 'collusion' hypothesis for the elevation of extracellular L-Glu in the early stages of inflammation. 1. Activated microglia release L-Glu. 2. The resultant elevation of extracellular L-Glu causes the elevation of astrocytic intracellular L-Glu. 3. The elevation of astrocytic intracellular L-Glu downregulates GLAST expression. 4. The decrease in GLAST expression further exacerbates the elevation of extracellular L-Glu.

Discussion

To quantify L-Glu transporter function, we measured the extracellular concentrations of L-Glu 30 min after a single exogenous application of L-Glu to the medium (the starting concentration was 100 μM). To limit any contributions of extra L-Glu from dying cells, and to verify a substantial contribution of the decrease in L-Glu transport potency to an elevated concentration of extracellular L-Glu in inflammation, we first determined the optimal conditions for inflammation without cell death. We used a lower concentration of LPS (10 ng/mL) than is generally used [35,36]. LPS application at a concentration of 10 ng/mL for 72 h activated the microglia but did not cause either LDH leakage or decreases in MTT reduction in the mixed culture, astrocyte pure culture, or microglia pure culture. LPS induces an inflammatory response in microglia via Toll-like receptor 4 (TLR4) [37]. TLR4 is also expressed by astrocytes, and astrocytes themselves have shown inflammatory responses in response to LPS in some reports [38]. In the present study, however, microglia were essential for the decreased L-Glu by astrocytes, and LPS did not affect L-Glu uptake in astrocyte cultures. Because the expression of TLR4 by astrocytes is less than that of microglia [37], the LPS stimulation in our model of inflammation without cell death may be insufficient to induce phenotypic changes in astrocytes. These mild inflammatory conditions may reflect the early stages of neuroinflammation *in vivo*, in which early microglial activation has been observed to precede the phenotypic changes in astrocytes [39].

In the present study, we pharmacologically confirmed that GLAST, and not GLT-1, was the predominant functional L-Glu transporter. We also confirmed that the expression level of GLT-1 is much lower than that of GLAST. GLT-1 has been reported to be functional in neuron-astrocyte co-cultures at 32 to 44 DIV [40]. This discrepancy most likely arises from the maturation stages of neurons, as the functional development of GLT-1 correlates with neuronal maturation [41]. The expression of GLAST was significantly decreased in the 'non-cell death inflammation model', which indicates that the decrease in L-Glu uptake in this inflammation model was mainly caused by the downregulation of GLAST.

Activated microglia release various soluble factors, including inflammatory cytokines [18,19], reactive oxygen species [20], NO [16], L-Glu [21,22], and ATP [23,24]. We demonstrated that L-Glu is the factor that downregulates GLAST in astrocytes during inflammation without cell death. Although activated microglia are known to release L-Glu through hemichannels [21,22], the neurological importance of this phenomenon remains unclear. We showed that the hemichannel inhibitor CBX completely suppressed the release of L-Glu from microglia, the decrease in L-Glu uptake, and the downregulation of GLAST expression during inflammation without cell death. These data provide strong evidence that L-Glu is the microglial releasing factor that downregulates GLAST. High concentrations of ATP have also been shown to downregulate GLAST through the P2X7 receptor [28]. However, we believe that ATP did not contribute to the down-regulation of GLAST in the inflammation model without cell death here because L-Glu uptake did not change when the astrocyte culture was treated with ATP (Figure 5A) or the P2X7 agonist BzATP (Figure 5B). We also confirmed that neither the P2X receptor antagonist TNP-ATP (Figure 5C) nor the P2X7-specific antagonist BBG (Figure 5D) inhibited the decrease in L-Glu uptake in this inflammation model. Other microglial releasing factors, such as TNF-α, IL-1β, and arachidonic acid, are also known to decrease the L-Glu transport in astrocyte cultures [25-27]. However, the conditioned media collected from our model of inflammation without cell death had no effect in the astrocyte culture. Because the LPS stimulation here was lower than that of other studies [35,36] (to prevent cell death), the amount of these factors in the conditioned media may have been insufficient to affect L-Glu transporters.

Recent reports have suggested that the expression of L-Glu transporters is regulated by L-Glu through metabotropic glutamate receptors (mGluRs), that is, the group I mGluR agonist downregulates GLAST, whereas the group II mGluR agonist has the opposite effect [42,43]. However, neither the group I mGluR agonist nor the group II mGluR agonist affected the expression of GLAST in the present study. Instead, we clarified that the elevation of intracellular L-Glu in astrocytes is important for the downregulation of GLAST as shown in Figure 8. It has been clarified that translation initiation is regulated by intracellular L-Glu transported by GLAST in Bergmann glial cells [44,45]. They also showed that mammalian target of rapamycin (mTOR), increase in intracellular Ca^{2+} levels, and p60(Src)/PI3K/PKB pathway are involved in this regulation. Further investigation is necessary to confirm whether the same pathways are involved in the downregulation of GLAST observed in our study. Of interest, a sustained elevation of extracellular L-Glu induced by the same protocol as Figure 6 did not cause the downregulation of glutamine synthetase (GS) in our preliminary experiment (data not shown), suggesting that this regulation is GLAST or L-Glu transporter-specific. The comparison of the upstream DNA sequences of GLAST and GS might provide useful information. Besides, in *Saccharomyces cerevisiae*, the activator (NIL1p) of the amino acid transporter is inactivated by increases in intracellular glutamate [46]. It is possible that a conserved mechanism similar to this also exist in astrocytes. Our findings strongly suggest that L-Glu is the microglial releasing factor which results in downregulation of GLAST in the early stage of inflammation. However, whether or not the quantity of L-Glu released from microglia is enough to induce a range of reaction still needs to be elucidated. Based on the discussion above, the co-factors to enhance the signaling pathway in the astrocytes leading to the downregulation of GLAST might be also released from microglia.

Conclusions

Our findings suggest that activated microglia trigger the elevation of extracellular L-Glu through their own release of L-Glu, astrocyte L-Glu transporters are downregulated by the elevation of astrocytic intracellular L-Glu, and further elevation of extracellular L-Glu is caused as an early event of neuroinflammation (Figure 9).

Abbreviations

ANOVA: Analysis of variance; ATP: Adenosine 5′-triphosphate disodium salt hydrate; BPB: Bromophenol blue sodium salt; BSA: Albumin bovine serum; BzATP: 2′ (3′)-O-(4-Benzoylbenzoyl)ATP triethylammonium salt; CBX: Carbenoxolone; CNS: Central nervous system; DHK: Dihydrokainic acid; DIV: Days *in vitro*; DMEM: Dulbecco's modified eagle medium; DNA: Deoxyribonucleic acid; EDTA: Ethylenediaminetetraacetate; EGTA: Ethyleneglycoldiaminetetraacetate; FBS: Fetal bovine serum; GFAP: Glial fibrillary acidic protein; GlDH: Glutamate dehydrogenase; HS: Horse serum; LDH: Lactate dehydrogenase; L-Glu: L-glutamate; LPS: Lipopolysaccharide; mGluRs: Metabotropic glutamate receptors; MPMS: 1-methoxy-5-methylphenazinium methyl sulfate; MTT: 3-(4,5-dimethyl-2-thiazolyl)-2,5-diphenyl-2H-tetrazolium bromide; β-NAD: β-nicotinamide adenine dinucleotide; NO: Nitric oxide; NP-40: Polyoxyethylene(9)octylphenyl ether; OxATP: Adenosine 5′-triphosphate periodate oxidized sodium salt; PBS: Phosphate-buffered saline; PFA: Paraformaldehyde; RNA: Ribonucleic acid; RT-PCR: Polymerase chain reaction; SD: Sprague–Dawley; SDS: Sodium dodecyl sulfate; TBOA: DL-threo-β-benzyloxyaspartic acid; TLR4: Toll-like receptor 4; TNP-ATP: 2′,3′-O-(2,4,6-Trinitrophenyl)ATP salt hydrate; Tris–HCl: Tris (hydroxymethyl) aminomethane; Tuj1: β3 tubulin; UCPH 101: 2-Amino-5,6,7,8-tetrahydro-4-(4-methoxyphenyl)-7-(naphthalen-1-yl)-5-oxo-4H-chromene-3-carbonitrile.

Competing interests

I declare that I have no significant competing financial, professional or personal interests that might have influenced the performance or presentation of the work described in this manuscript.

Authors' contributions

JT performed experimental work and manuscript writing. KF performed experimental work. MM performed additional experimental work. TS provided advice on the experimental direction. YS provided advice on manuscript writing and preparation. KS designed the biological experimental plan and performed biological experiments, data analysis, manuscript writing, and preparation. All authors have read and approved the final version of the manuscript.

Acknowledgements
This study was partly supported by a Grant-in-Aid from the Food Safety Commission of Japan (No. 1003); a Grant-in-Aid for Young Scientists from MEXT, Japan (KAKENHI 21700422); the Program for the Promotion of Fundamental Studies in Health Sciences of NIBIO, Japan; a Health and Labor Science Research Grant for Research on Risks of Chemicals; and a Health and Labor Science Research Grant for Research on New Drug Development from MHLW, Japan, awarded to KS and YS.

Author details
[1]Laboratory of Neuropharmacology, Division of Pharmacology, National Institute of Health Sciences, 1-18-1 Kamiyoga, Setagaya-ku, Tokyo 158-8501, Japan. [2]Division of Basic Biological Science, Faculty of Pharmacy, Keio University, 1-5-30 Shiba-koen, Minato-ku, Tokyo 105-8512, Japan.

Received: 25 May 2012 Accepted: 1 December 2012
Published: 23 December 2012

References

1. Kumar A, Singh RL, Babu GN: **Cell death mechanisms in the early stages of acute glutamate neurotoxicity.** *Neurosci Res* 2010, **66**:271–278.
2. Choi DW: **Glutamate neurotoxicity and diseases of the nervous system.** *Neuron* 1988, **1**:623–634.
3. Rothstein JD, Dykes-Hoberg M, Pardo CA, Bristol LA, Jin L, Kuncl RW, Kanai Y, Hediger MA, Wang Y, Schielke JP, Welty DF: **Knockout of glutamate transporters reveals a major role for astroglial transport in excitotoxicity and clearance of glutamate.** *Neuron* 1996, **16**:675–686.
4. Lauderback CM, Harris-White ME, Wang Y, Pedigo NW Jr, Carney JM, Butterfield DA: **Amyloid beta-peptide inhibits Na^+-dependent glutamate uptake.** *Life Sci* 1999, **65**:1977–1981.
5. Rothstein JD: **Excitotoxicity and neurodegeneration in amyotrophic lateral sclerosis.** *Clin Neurosci* 1995–1996, **3**:348–359.
6. Choudary PV, Molnar M, Evans SJ, Tomita H, Li JZ, Vawter MP, Myers RM, Bunney WE Jr, Akil H, Watson SJ, Jones EG: **Altered cortical glutamatergic and GABAergic signal transmission with glial involvement in depression.** *Proc Natl Acad Sci USA* 2005, **102**:15653–15658.
7. Beart PM, O'Shea RD: **Transporters for L-glutamate: an update on their molecular pharmacology and pathological involvement.** *Br J Pharmacol* 2007, **150**:5–17.
8. Guo F, Sun F, Yu JL, Wang QH, Tu DY, Mao XY, Liu R, Wu KC, Xie N, Hao LY, Cai JQ: **Abnormal expressions of glutamate transporters and metabotropic glutamate receptor 1 in the spontaneously epileptic rat hippocampus.** *Brain Res Bull* 2010, **81**:510–516.
9. Rakhade SN, Loeb JA: **Focal reduction of neuronal glutamate transporters in human neocortical epilepsy.** *Epilepsia* 2008, **49**:226–236.
10. Proper EA, Hoogland G, Kappen SM, Jansen GH, Rensen MG, Schrama LH, van Veelen CW, van Rijen PC, van Nieuwenhuizen O, Gispen WH, de Graan PND: **Distribution of glutamate transporters in the hippocampus of patients with pharmaco-resistant temporal lobe epilepsy.** *Brain* 2002, **125**:32–43.
11. Ward RJ, Colivicchi MA, Allen R, Schol F, Lallemand F, de Witte P, Ballini C, Corte LD, Dexter D: **Neuro-inflammation induced in the hippocampus of 'binge drinking' rats may be mediated by elevated extracellular glutamate content.** *J Neurochem* 2009, **111**:1119–1128.
12. Castillo J, Dávalos A, Alvarez-Sabín J, Pumar JM, Leira R, Silva Y, Montaner J, Kase CS: **Molecular signatures of brain injury after intracerebral hemorrhage.** *Neurology* 2002, **58**:624–629.
13. Allen NJ, Barres BA: **Neuroscience: Glia - more than just brain glue.** *Nature* 2009, **457**:675–677.
14. Lehnardt S: **Innate immunity and neuroinflammation in the CNS: the role of microglia in Toll-like receptor-mediated neuronal injury.** *Glia* 2010, **58**:253–263.
15. Perry VH, Nicoll JA, Holmes C: **Microglia in neurodegenerative disease.** *Nat Rev Neurol* 2010, **6**:193–201.
16. Kreutzberg GW: **Microglia: a sensor for pathological events in the CNS.** *Trends Neurosci* 1996, **19**:312–318.
17. Lynch MA: **The multifaceted profile of activated microglia.** *Mol Neurobiol* 2009, **40**:139–156.
18. Hanisch UK: **Microglia as a source and target of cytokines.** *Glia* 2002, **40**:140–155.
19. Nakajima K, Kohsaka S: **Microglia: activation and their significance in the central nervous system.** *J Biochem* 2001, **130**:169–175.
20. Block ML, Hong JS: **Chronic microglial activation and progressive dopaminergic neurotoxicity.** *Biochem Soc Trans* 2007, **35**:1127–1132.
21. Takeuchi H, Jin S, Wang J, Zhang G, Kawanokuchi J, Kuno R, Sonobe Y, Mizuno T, Suzumura A: **Tumor necrosis factor-alpha induces neurotoxicity via glutamate release from hemichannels of activated microglia in an autocrine manner.** *J Biol Chem* 2006, **281**:21362–21368.
22. Yawata I, Takeuchi H, Doi Y, Liang J, Mizuno T, Suzumura A: **Macrophage-induced neurotoxicity is mediated by glutamate and attenuated by glutaminase inhibitors and gap junction inhibitors.** *Life Sci* 2008, **82**:1111–1116.
23. Higashi Y, Segawa S, Matsuo T, Nakamura S, Kikkawa Y, Nishida K, Nagasawa K: **Microglial zinc uptake via zinc transporters induces ATP release and the activation of microglia.** *Glia* 2011, **59**:1933–1945.
24. Kim SY, Moon JH, Lee HG, Kim SU, Lee YB: **ATP released from beta-amyloid-stimulated microglia induces reactive oxygen species production in an autocrine fashion.** *Exp Mol Med* 2007, **39**:820–827.
25. Carmen J, Rothstein JD, Kerr DA: **Tumor necrosis factor-alpha modulates glutamate transport in the CNS and is a critical determinant of outcome from viral encephalomyelitis.** *Brain Res* 2009, **1263**:143–154.
26. Prow NA, Irani DN: **The inflammatory cytokine, interleukin-1 beta, mediates loss of astroglial glutamate transport and drives excitotoxic motor neuron injury in the spinal cord during acute viral encephalomyelitis.** *J Neurochem* 2008, **105**:1276–1286.
27. Volterra A, Trotti D, Racagni G: **Glutamate uptake is inhibited by arachidonic acid and oxygen radicals via two distinct and additive mechanisms.** *Mol Pharmacol* 1994, **46**:986–992.
28. Liu YP, Yang CS, Chen MC, Sun SH, Tzeng SF: **Ca(2+)-dependent reduction of glutamate aspartate transporter GLAST expression in astrocytes by P2X(7) receptor-mediated phosphoinositide 3-kinase signaling.** *J Neurochem* 2010, **113**:213–227.
29. Sato K, Matsuki N, Ohno Y, Nakazawa K: **Estrogens inhibit l-glutamate uptake activity of astrocytes via membrane estrogen receptor alpha.** *J Neurochem* 2003, **86**:1498–1505.
30. Sato K, Saito Y, Oka J, Ohwada T, Nakazawa K: **Effects of tamoxifen on L-glutamate transporters of astrocytes.** *J Pharmacol Sci* 2008, **107**:226–230.
31. Nakajima K, Shimojo M, Hamanoue M, Ishiura S, Sugita H, Kohsaka S: **Identification of elastase as a secretory protease from cultured rat microglia.** *J Neurochem* 1992, **58**:1401–1408.
32. Kohl A, Dehghani F, Korf HW, Hailer NP: **The bisphosphonate clodronate depletes microglial cells in excitotoxically injured organotypic hippocampal slice cultures.** *Exp Neurol* 2003, **181**:1–11.
33. Abe K, Matsuki N: **Measurement of cellular 3-(4,5-dimethylthiazol-2-yl)-2,5-diphenyltetrazolium bromide (MTT) reduction activity and lactate dehydrogenase release using MTT.** *Neurosci Res* 2000, **38**:325–329.
34. Wink MR, Braganhol E, Tamajusuku AS, Lenz G, Zerbini LF, Libermann TA, Sévigny J, Battastini AM, Robson SC: **Nucleoside triphosphate diphosphohydrolase-2 (NTPDase2/CD39L1) is the dominant ectonucleotidase expressed by rat astrocytes.** *Neuroscience* 2006, **138**:421–432.
35. Li J, Ramenaden ER, Peng J, Koito H, Volpe JJ, Rosenberg PA: **Tumor necrosis factor alpha mediates lipopolysaccharide-induced microglial toxicity to developing oligodendrocytes when astrocytes are present.** *J Neurosci* 2008, **28**:5321–5330.
36. Bal-Price A, Brown GC: **Inflammatory neurodegeneration mediated by nitric oxide from activated glia-inhibiting neuronal respiration, causing glutamate release and excitotoxicity.** *J Neurosci* 2001, **21**:6480–6491.
37. Lehnardt S, Lachance C, Patrizi S, Lefebvre S, Follett PL, Jensen FE, Rosenberg PA, Volpe JJ, Vartanian T: **The toll-like receptor TLR4 is necessary for lipopolysaccharide-induced oligodendrocyte injury in the CNS.** *J Neurosci* 2002, **22**:2478–2486.
38. Carpentier PA, Begolka WS, Olson JK, Elhofy A, Karpus WJ, Miller SD: **Differential activation of astrocytes by innate and adaptive immune stimuli.** *Glia* 2005, **49**:360–374.
39. Tilleux S, Hermans E: **Neuroinflammation and regulation of glial glutamate uptake in neurological disorders.** *J Neurosci Res* 2007, **85**:2059–2070.
40. Swanson RA, Liu J, Miller JW, Rothstein JD, Farrell K, Stein BA: **Longuemare MC: Neuronal regulation of glutamate transporter subtype expression in astrocytes.** *J Neurosci* 1997, **17**:932–940.

41. Perego C, Vanoni C, Bossi M, Massari S, Basudev H, Longhi R, Pietrini G: **The GLT1 and GLAST glutamate transporters are expressed on morphologically distinct astrocytes and regulated by neuronal activity in primary hippocampal cocultures.** *J Neurochem* 2000, **75**:1076–1084.
42. Gegelashvili G, Dehnes Y, Danbolt NC, Schousboe A: **The high-affinity glutamate transporters GLT1, GLAST, and EAAT4 are regulated via different signalling mechanisms.** *Neurochem Int* 2000, **37**:163–170.
43. Aronica E, Gorter JA, Ijlst-Keizers H, Rozemuller AJ, Yankaya B, Leenstra S, Troost D: **Expression and functional role of mGluR3 and mGluR5 in human astrocytes and glioma cells: opposite regulation of glutamate transporter proteins.** *Eur J Neurosci* 2003, **17**:2106–2118.
44. González-Mejía ME, Morales M, Hernández-Kelly LC, Zepeda RC, Bernabé A, Ortega A: **Glutamate-dependent translational regulation in cultured Bergmann glia cells: involvement of p70S6K.** *Neuroscience* 2006, **141**:1389–1398.
45. Zepeda RC, Barrera I, Castelán F, Suárez-Pozos E, Melgarejo Y, González-Mejía E, Hernández-Kelly LC, Lopez-Bayghen E, Aguilera J, Ortega A: **Glutamate-dependent phosphorylation of the mammalian target of rapamycin (mTOR) in Bergmann glial cells.** *Neurochem Int* 2009, **55**:282–287.
46. Stanbrough M, Rowen DW, Magasanik B: **Role of the GATA factors Gln3p and Nil1p of Saccharomyces cerevisiae in the expression of nitrogen-regulated genes.** *Proc Natl Acad Sci USA* 1995, **92**:9450–9454.

doi:10.1186/1742-2094-9-275
Cite this article as: Takaki *et al.*: L-glutamate released from activated microglia downregulates astrocytic L-glutamate transporter expression in neuroinflammation: the 'collusion' hypothesis for increased extracellular L-glutamate concentration in neuroinflammation. *Journal of Neuroinflammation* 2012 9:275.

Research article

Drug Testing and Analysis

Received: 2 August 2011 Revised: 11 January 2012 Accepted: 13 January 2012 Published online in Wiley Online Library: 8 March 2012

(www.drugtestinganalysis.com) DOI 10.1002/dta.1327

Rapid enantiomeric separation and simultaneous determination of phenethylamines by ultra high performance liquid chromatography with fluorescence and mass spectrometric detection: application to the analysis of illicit drugs distributed in the Japanese market and biological samples

Shinsuke Inagaki,[a] Haruo Hirashima,[a] Sayuri Taniguchi,[a] Tatsuya Higashi,[a] Jun Zhe Min,[a] Ruri Kikura-Hanajiri,[b] Yukihiro Goda[b] and Toshimasa Toyo'oka[a]*

A rapid enantiomeric separation and simultaneous determination method based on ultra high performance liquid chromatography (UHPLC) was developed for phenethylamine-type abused drugs using (*R*)-(−)-4-(*N*,*N*-dimethylaminosulfonyl)-7-(3-isothiocyanatopyrrolidin-1-yl)-2,1,3-benzoxadiazole ((*R*)-(−)-DBD-Py-NCS) as the chiral fluorescent derivatization reagent. The derivatives were rapidly enantiomerically separated by reversed-phase UHPLC using a column of 2.3-μm octadecylsilica (ODS) particles by isocratic elution with water–methanol or water–acetonitrile systems as the mobile phase. The proposed method was applied to the analysis of products containing illicit drugs distributed in the Japanese market. Among the products, 1-(3,4-methylenedioxyphenyl)butan-2-amine (BDB) and 1-(2-methoxy4,5-methylenedioxyphenyl)propan-2-amine (MMDA-2) were detected in racemic form. Furthermore, the method was successfully applied to the analysis of hair specimens from rats that were continuously dosed with diphenyl(pyrrolidin-2-yl)methanol (D2PM). Using UHPLC-fluorescence (FL) detection, (*R*)- and (*S*)-D2PM from hair specimens were enantiomerically separated and detected with high sensitivity. The detection limits of (*R*)- and (*S*)-D2PM were 0.12 and 0.21 ng/mg hair, respectively (signal-to-noise ratio (S/N) = 3).

Keywords: phenethylamines; diphenyl(pyrrolidin-2-yl)methanol (D2PM); (*R*)-(−)-DBD-Py-NCS; chiral derivatization method; ultra high performance liquid chromatography (UHPLC)

Introduction

Health hazards caused by the abuse of illicit drugs occur frequently among young people and have become a serious concern. Such drugs are easily obtainable via the Internet, adult shops, street markets, and so on. The use of illicit drugs is also the gateway to narcotic and psychostimulant drugs abuse. In Japan, the Pharmaceutical Affairs Law was revised, and the regulation was tightened by introducing a system of controlled substances, designated as Shitei-Yakubutsu, in April 2007 (31 compounds and 1 plant).[1,2] Under this Act, compounds that have potential harmful health effects are designated Shitei-Yakubutsu, and rapid response to such compounds is facilitated. This system temporarily decreased the distribution of designated substances in Japan. However, due to synthetic modification, structural analogs of designated compounds may slip past regulations. As of August 2011, 60 substances (classified as 26 phenethylamines, 12 tryptamines, 6 alkyl nitrites, 4 piperazines, 10 cannabinoids, 1 diterpene, and 1 plant) are listed as designated substances; the list is continually revised and improved as necessary. Diphenyl(pyrrolidin-2-yl)methanol (D2PM), and 1-(2-fluorophenyl)-*N*-methylpropan-2-amine (*N*-methyl-2FMP), were recently added to the designated substances list; there is concern that analogs of these substances may be distributed as new illicit drugs. In particular, D2PM and its analogs are organocatalysts used for various asymmetric syntheses; however, such chemical reagents are

* *Correspondence to: Toshimasa Toyo'oka, Laboratory of Analytical and Bio-Analytical Chemistry, School of Pharmaceutical Sciences, and Global COE Program, University of Shizuoka, 52–1 Yada, Suruga-ku, Shizuoka 422–8526, Japan. E-mail: toyooka@u-shizuoka-ken.ac.jp*

a *Laboratory of Analytical and Bio-Analytical Chemistry, School of Pharmaceutical Sciences, and Global COE Program, University of Shizuoka, Japan*

b *Division of Pharmacognosy, Phytochemistry and Narcotics, National Institute of Health Sciences, Tokyo, Japan*

likely abused.[3–7] To prevent distribution of these substances, it is crucial to establish an analytical method of detection before they enter the Japanese market. Therefore, development of simple and rapid screening methods of illicit drugs and their structurally related compounds is required.

Most phenethylamine compounds are chiral, and their enantiomers can possess different pharmacological activities and pharmacokinetic/pharmacodynamic properties. For example, it is well known that the enantiomers of methamphetamine and amphetamine differ in their biological and metabolic activities. The *d*-isomer has the greatest biological activity, whereas the *l*-isomer is far less active.[8,9] Therefore, it is important to ensure enantiomeric purity by chiral separation. Furthermore, relevant information can be gathered by indentifying the manufacturing method, the producer countries, and their sources by analyzing impurities and determining of the ratio of optical isomers in the distributed illicit drugs.

Numerous strategies for enantiomeric separation of chiral compounds are available using various separation techniques such as gas chromatography (GC), high performance liquid chromatography (HPLC), supercritical fluid chromatography (SFC), capillary electrophoresis (CE), and capillary electrochromatography (CEC).[10–18] Among these methods, HPLC is one of the most effective tools for chiral separation. The methods are divided into three broad classes: chiral stationary phase (CSP) methods, chiral mobile phase methods, and chiral derivatization methods.[15–17] CSP methods use packing materials combined with chiral molecules at the carrier surface as the stationary phase. A number of CSP methods have already been developed and are widely used. However, to perform chiral separations of target enantiomers by HPLC, the CSP must be selected through a trial-and-error process based solely on prior experience. Chiral mobile phase methods form a diastereomer complex by passing the sample through a column using a mobile phase containing chiral molecules. This method does not require the column to be packed with chiral molecules or complicated handling; however, the kinds of enantiomers that can be separated using this method are limited. Indeed, direct chromatographic separation using hydroxypropyl-β-cyclodextrin (HP-β-CD) as a chiral mobile phase additive has been investigated for the chiral separation of amphetamine and its derivatives; baseline separations could not be achieved because of the peak broadening.[19] These basic compounds tend to broaden peaks in consequence of residual silanol in the column. On the other hand, the chiral derivatization method does not require the comparatively expensive analytical column containing a CSP, and analysis can be performed using a conventional HPLC column such as an ODS column. Guillame *et al.* reported that *N*-α-(2,4-dinitro-5-fluorophenyl)-L-alaninamide (Marfey's reagent) and 2,3,4-tri-O-acetyl-α-D-arabinopyranosyl isothiocyanate (AITC) would be effective for enantiomeric separation of amphetamine, its derivatives, and several β-blockers (atenorol, propranorol, and so on) using HPLC–UV.[19] Furthermore, using a fluorescence derivatization method such as HPLC-fluorescence (HPLC-FL) detection has the advantage of highly sensitive detection.

In our previous study, we reported an HPLC-FL method for the enantiomeric separation of D2PM and psychotropic methylphenidate (MPH) using a chiral fluorescent derivatization reagent, (*R*)-(−)-4-(*N*,*N*-dimethylaminosulfonyl)-7-(3-isothiocyanatopyrrolidin-1-yl)-2,1,3-benzoxadiazole ((*R*)-(−)-DBD-Py-NCS).[20] However, to the best of our knowledge, the method and the reagent have not been applied for the analysis of other drugs.

In this study, we conducted to develop a method for rapid enantiomeric separation and simultaneous determination of phenethylamine-type abused drugs and established a detection method using UHPLC-FL and electrospray ionization time-of-flight mass spectrometry (ESI-TOF-MS). UHPLC is an analytical technique developed in the last half decade that is an extension of conventional HPLC techniques; it uses small particles in the separation column and pumping of the mobile phase under ultra-high pressure conditions.[21–23] Application to the analysis of phenethylamine drugs distributed on the Japanese market and the analysis of rat-hair specimens after oral dose of racemic, (*R*)-, and (*S*)-D2PM are also discussed.

Experimental

Materials and reagents

The hydrochloric acid salts of racemic phenethylamines, i.e. 1-(3,4-methylenedioxyphenyl)butan-2-amine (BDB), 1-(4-iodo-2,5-dimethoxyphenyl)propan-2-amine (DOI), 2-ethylamino-1-phenylpropan-1-one (*N*-ethylcatinone), 1-(4-fluorophenyl)propan-2-amine (4-FMP), 2-methylamino-1-(3,4-methylenedioxyphenyl)butan-1-one (bk-MBDB), 2-ethylamino-1-(3,4-methylenedioxyphenyl)propan-1-one (bk-MDEA), 1-(2-fluorophenyl)-*N*-methylpropan-2-amine (*N*-methyl-2FMP), 2-(methylamino)-1-(4-methylphenyl)propan-1-one (4-methylmethocatinone), 1-(2-methoxy4, 5-methylenedioxyphenyl)propan-2-amine (MMDA-2), and 1-(4-methoxyphenyl)-*N*-methylpropan-2-amine (PMMA) were obtained from the National Institutes of Health Sciences (NIHS, Tokyo, Japan). Products sold in the past as legal substances on the Japanese market were used for the determination of the phenethylamine-type abused drugs. Racemic methylphenidate hydrochloride (MPH), (2R,2′R)-(+)-*threo*-methyl α-phenyl-α-(2-piperidyl)acetate hydrochloride (D-MPH), (2S,2′S)-(−)-*threo*-methyl α-phenyl-α-(2-piperidyl)acetate hydrochloride (L-MPH), and leucine enkephalin were purchased from Sigma-Aldrich Chemical Co. (St Louis, MO, USA). (*R*)-Diphenyl(pyrrolidin-2-yl)methanol ((*R*)-(+)-α,α-diphenyl-2-pyrrolidinemethanol, (*R*)-D2PM), (*S*)-diphenyl(pyrrolidin-2-yl)methanol ((*S*)-(−)-α,α-diphenyl-2-pyrrolidinemethanol, (*S*)-D2PM), α-(4-piperidyl)benzhydrol (PBH as internal standard), (*R*)-(−)-4-(*N*,*N*-dimethylaminosulfonyl)-7-(3-isothiocyanatopyrrolidin-1-yl)-2,1,3-benzoxadiazole ((*R*)-(−)-DBD-Py-NCS), (*R*)-(+)-4-nitro-7-(2-chloroformylpyrrolidin-1-yl) -2,1,3-benzoxadiazole ((*R*)-(+)-NBD-Pro-COCl), 2,3,4,6-tetra-*O*-acetyl-β-D-glucopyranosyl isothiocyanate (GITC), and triethylamine were obtained from Tokyo Kasei Co. (Tokyo, Japan). Diethyl ether, dimethyl sulfoxide (DMSO), and trifluoroacetic acid (TFA) were obtained from Kanto Kagaku Co. (Tokyo, Japan). Sodium dodecyl sulfate (SDS) and hydrochloric acid (HCl) were purchased from Wako Pure Chemicals (Osaka, Japan). Acetonitrile (CH_3CN), methanol (CH_3OH), and formic acid (FA) were of LC–MS grade (Wako Pure Chemicals, Osaka, Japan). Saline was purchased from Otsuka Pharmaceutical Factory, Inc. (Naruto, Japan). All other reagents were of analytical-reagent grade and were used without further purification.

UHPLC-FL and ESI-TOF-MS conditions

A Shimadzu (Kyoto, Japan) ultra-fast liquid chromatograph system consisting of two LC-20AD pumps, a degasser (DGU-20A_3) and an auto-injector (SIL-20AC_{HT}) was used. Reversed-phase liquid chromatography was performed using TSK-gel ODS-140HTP column (2.1 mm i.d. × 100 mm, 2.3 μm, Tosoh, Tokyo). The column

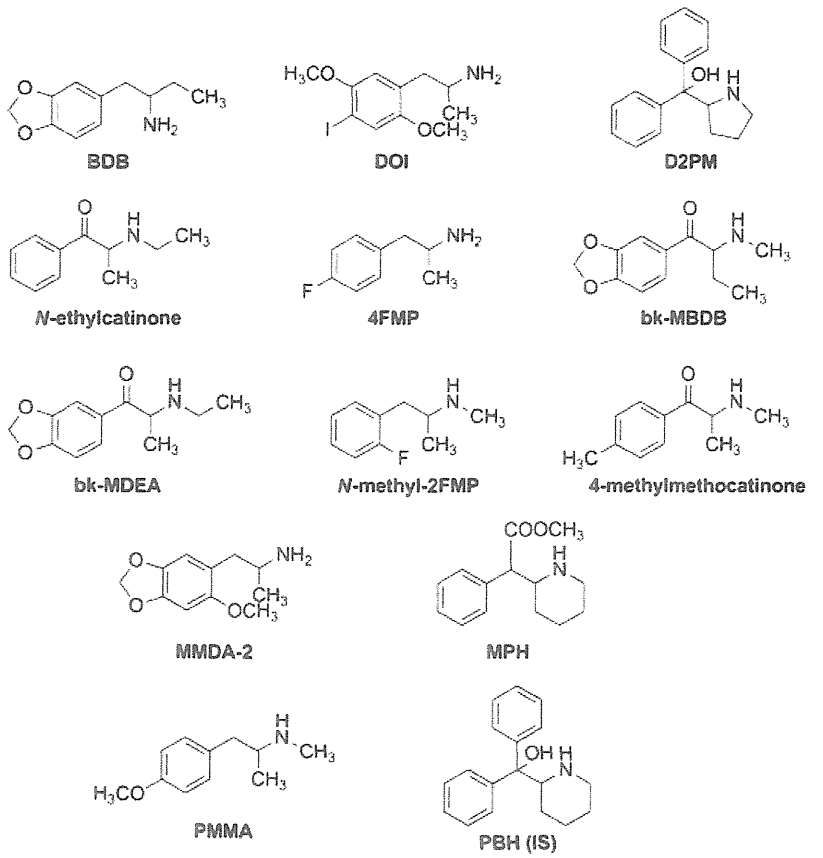

Figure 1. Chemical structures of phenethylamines used in this study.

Table 1. Separation factor (α) and resolution factor (R_s) for enantiomeric resolution of (*R*)- and (*S*)-D2PM using the chiral derivatization method[a]

Chiral derivatization reagents	α	R_s
(*R*)-(−)-DBD-Py-NCS	1.190	3.450
(*R*)-(+)-NBD-Pro-COCl	0.244	0.888
GITC	1.070	1.420

[a]Mobile phase: H_2O–CH_3OH–FA (45:55:0.1, v/v/v).

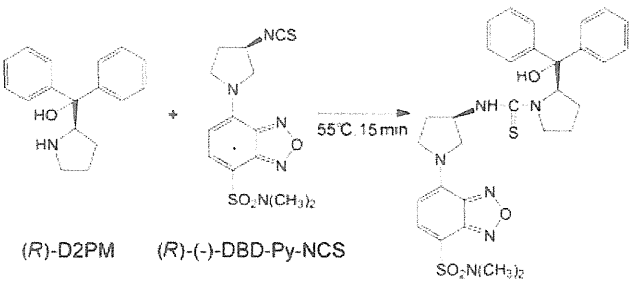

Figure 2. Derivatization reaction of (*R*)-D2PM with (*R*)-(−)-DBD-Py-NCS.

was maintained at 40°C. The eluent was monitored by an RF-10A_{XL} fluorescence detector (Shimadzu). The wavelengths of the fluorescence detector were set at 450 nm (excitation) and 560 nm (emission). The flow rate of the mobile phase was 0.45 ml/min. Isocratic separations were achieved using H_2O–CH_3OH–FA (40:60:0.1 or 45:55:0.1, *v/v/v*) as the mobile phase unless otherwise mentioned. The injection volume was fixed at 2 µl.

ESI-TOF-MS detection was performed using a Waters LCT Premier XE mass spectrometer (Waters, Milford, MA, USA). The profile data for positive ions of *m/z* 100–1000 were recorded (W-mode, mass resolution: 1.0×10^4). The capillary voltage was set at 3000 V, while the cone voltage was 10 V. Nitrogen was used as the drying gas. The desolvation gas flow rate was 650 L/h, and the cone gas flow rate was maintained at 50 L/h. The desolvation temperature was 350°C, and the source temperature was 120°C. A lock-mass of leucine enkephalin at a concentration of 2 ng/ml in H_2O–CH_3CN–FA (50:50:0.1, *v/v/v*) for the positive ion mode ($[M+H]^+ = 556.2771$) was used at a flow rate of 5 µl/min via a lock-spray ionization source. Data were collected in the centroid mode, the lock spray frequency was set at 5 s, and the lock-mass data were averaged over 10 scans for correction.

Derivatization of phenethylamines by (R)-(−)-DBD-Py-NCS

One hundred microlitres of 2 mM (*R*)-(−)-DBD-Py-NCS in CH_3CN and 5 µl of triethylamine were added to 100 µl of the sample solution containing phenethylamines (0–10 µM) in H_2O–CH_3CN (50:50, *v/v*). The mixture was heated at 55°C for 15 min.[20] The solution was cooled at 5°C, and an aliquot (2 µl) was injected into the UHPLC-FL and ESI-TOF-MS systems.

Analysis of phenethylamines from the products distributed in the Japanese market

The products distributed in the past as legal substances on the Japanese market were enantiomerically separated and analyzed for determination of phenethylamines. Product 1 (labelled as BDB, yellow powder, 1 mg) was dissolved in 1 ml of H_2O–CH_3OH (1:1, *v/v*), and product 2 (labelled as Honey Flash 2, colourless liquid) was diluted 10 times with H_2O–CH_3OH (1:1, *v/v*). The solution was sonicated for 10 min and then centrifuged at 500×g for 10 min. After centrifugation, 100 µl of the supernatant was derivatized by (*R*)-(−)-DBD-Py-NCS using the same procedure described above, and the supernatant was filtered through a Millex-LG filter (0.20 µm, 4 mm i.d.; Nihon Millipore, Tokyo, Japan). The solution was cooled at 5°C, and an aliquot (2 µl) was injected into the UHPLC–ESI-TOF-MS systems.

Experimental animals

Healthy male Dark-Agouti (DA) rats (5 weeks old) were purchased from Japan SLC, Inc. (Hamamatsu, Japan). Animal care and experiments were conducted according to the guidelines for the care and use of laboratory animals of the University of Shizuoka. The rats were housed at a constant temperature (24 ± 1°C) with an alternating 12-h light/dark cycle with free access to food and water. Racemic (*R/S* ratio =1/1), (*R*)-, and (*S*)-D2PM dissolved in saline containing 5% (*v/v*) DMSO and 0.1 M HCl were orally administered to the rats for three weeks (40 mg/kg day). The control rats were orally administered saline instead of D2PM. One week after cessation of D2PM administration, hair specimens were collected from the rats. The collected hairs were washed with 1 ml of 0.1% SDS for 1 min by vortex mixing. After three rinses with distilled water in the same manner, the hair

Table 2. Retention time (t_R), separation factor (α), and resolution factor (R_s) for enantiomeric resolution of phenethylamines using (*R*)-(−)-DBD-Py-NCS as chiral derivatization reagent

Samples	*m/z* ([M + H]$^+$)	Mobile phase[a]	t_R (min)	α	R_s
BDB	547.1797	A	4.48, 4.87	1.10	1.53
DOI	675.0920	B	17.92, 18.44	1.03	0.70
D2PM	607.2161	A	12.15, 14.52	1.19	3.45
N-Ethylcatinone	531.1848	B	13.28, 16.53	1.25	5.69
4FMP	507.1648	A	4.49, 4.79	1.07	1.24
bk-MBDB	575.1746	A	5.55, 6.83	1.16	3.84
bk-MDEA	575.1746	A	6.13, 7.58	1.25	4.43
N-Methyl-2FMP	521.1805	B	12.46, 13.15	1.06	1.40
4-Methylmethocatinone	531.1848	A	7.91, 10.02	1.28	5.28
MMDA-2	563.1746	B	6.41, 6.69	1.05	1.02
MPH	587.2110	A	8.38, 9.38	1.13	2.50
PMMA	533.2005	A	4.26, 4.52	1.07	1.13

[a]A: H_2O–CH_3OH–FA (45:55:0.1, *v/v/v*); B: H_2O–CH_3CN–FA (62:38:0.1, *v/v/v*).

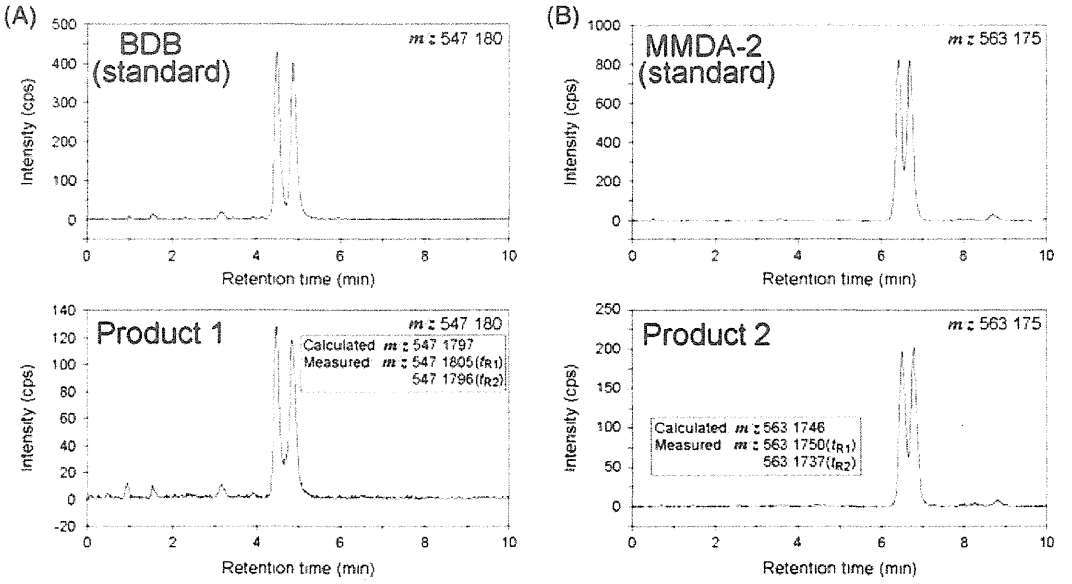

Figure 3. Typical chromatograms obtained from real products containing phenethylamines by UHPLC–ESI-TOF-MS. Analyte: (A) product 1 (yellow powder); (B) product 2 (colourless liquid). Mobile phase: (A) H_2O–CH_3OH–FA (45:55:0.1, *v/v/v*); (B) H_2O–CH_3CN–FA (62:38:0.1, *v/v/v*). Other conditions are described in Experimental section.

specimens were dried in air. The dried hairs were then cut into small pieces (approximately 2–3 mm) with scissors.

Acidic methanol extraction

A washed hair specimen (10 mg) was precisely weighed into a polypropylene tube, and 1.5 ml of CH_3OH–TFA (50:1, *v/v*) containing 5 μM of PBH as the internal standard was added for extraction. After sonication for 1 h, the solutions were allowed to stand overnight at room temperature. One millilitre of the supernatant was transferred into another tube and evaporated to dryness under a gentle stream of nitrogen at 40°C. Next, 50 μl of H_2O–CH_3CN (50:50, v/v) and 3 μl of triethylamine were serially added to the tube and reacted with 50 μl of (*R*)-(−)-DBD-Py-NCS in CH_3CN. The reaction mixture was heated at 55°C for 15 min. The supernatant was then filtered using a Millex-LG filter, and an aliquot of the filtrate (2 μl) was injected into the UHPLC-FL system.

Calibration curves and method validation by UHPLC-FL

Calibration curves were obtained by spiking a series of extraction solvents containing blank rat hair with (*R*)- and (*S*)-D2PM to give concentrations of 1.8–880 ng/mg hair. The curves were constructed by plotting the peak area ratios of (*R*)-D2PM and (*S*)-D2PM relative to the internal standard against the injected amounts. The curves were plotted for five different concentrations. Positive control hair specimens (QCL and QCH: quality control for low and high concentration, respectively) were prepared from the drug-free hair specimens according to a reported protocol with some modifications of drug concentrations,

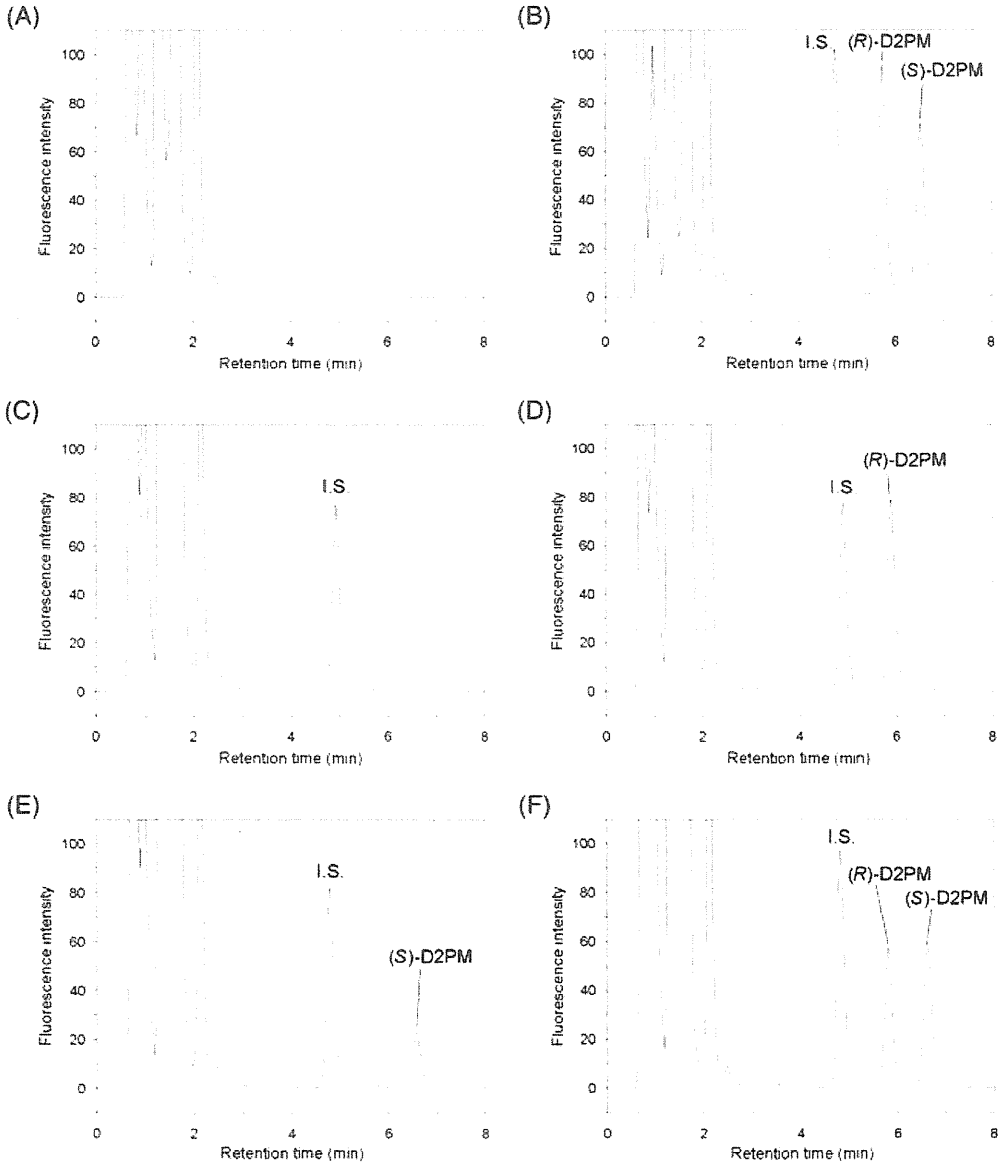

Figure 4. Typical chromatograms obtained from blank rat hair extract without addition of internal standard (A); rat hair extract spiked with 5 μmol/L (*R*)-D2PM and (*S*)-D2PM (B); rat hair extract following saline dose (C); (*R*)-D2PM (D); (*S*)-D2PM (E); and (*R,S*)-D2PM (F) by UHPLC–FL. Mobile phase: H_2O–CH_3OH–FA (40:60:0.1, v/v/v). Conditions of FL are described in Experimental section, and other conditions are the same as those in Figure 3.

Table 3. Intra- and inter-day validations of UHPLC-FL analysis of (*R*)- and (*S*)-D2PM from rat hair specimens

Samples	(*R*)-D2PM		(*S*)-D2PM	
	Amount (ng/mg hair, mean ± SD)	CV (%)	Amount (ng/mg hair, mean ± SD)	CV (%)
Intra-day assay ($n = 5$)				
QCL	051.6 ± 1.93	3.74	053.9 ± 3.52	6.53
QCH	408.1 ± 11.1	2.73	432.3 ± 28.2	6.52
Inter-day assay ($n = 5$)				
QCL	052.3 ± 3.16	6.05	052.0 ± 2.13	4.11
QCH	395.7 ± 26.3	6.64	400.9 ± 20.3	5.05

SD: standard deviation; CV: coefficient of variation.

Table 4. Amounts of (*R*)- and (*S*)-D2PM detected from rat hair by UHPLC-FL

Rat	Drug dose	Amounts of D2PM detected from rat hair (ng/mg hair, mean ± SD, $n = 5$)	
		(*R*)-D2PM	(*S*)-D2PM
1	(*R*)-D2PM	195.52 ± 9.69	Not detected
2	(*R*)-D2PM	073.89 ± 4.51	Not detected
3	(*S*)-D2PM	Not detected	133.61 ± 8.370
4	(*S*)-D2PM	Not detected	052.67 ± 2.010
5	*racemic*-D2PM	125.39 ± 7.53	187.91 ± 12.63
6	*racemic*-D2PM	052.06 ± 6.40	080.26 ± 10.98
7	–[a]	Not detected	Not detected
8	–[a]	Not detected	Not detected

[a]The rats were administered saline instead of D2PM.

soaking period, and rinse procedures.[24–26] Analyses were repeated five times a day and between days, and the precision (CVs, %) of intra- and inter-day assays was evaluated.

Results and discussion

Enantiomeric separation of phenethylamines using a chiral derivatization method

Figure 1 shows the chemical structures of phenethylamine-type abused drugs used in this study. We attempted to achieve rapid and simultaneous enantiomeric separation using a chiral fluorescent derivatization reagent, (*R*)-(−)-DBD-Py-NCS. In previous studies, (*R*)-(−)- and (*S*)-(+)-DBD-Py-NCS have proven to be very effective for total resolution of racemic mixtures of amino acids and thiol compounds by HPLC-FL.[27–29] The derivatization scheme for (*R*)-D2PM with (*R*)-(−)-DBD-Py-NCS is shown in Figure 2. Table 1 lists the separation factor (α) and resolution factor (R_s) for enantiomeric resolution of (*R*)- and (*S*)-D2PM using (*R*)-(−)-DBD-Py-NCS, (*R*)-(+)-NBD-Pro-COCl, and GITC as chiral derivatization reagents. The best resolution between the enantiomers was obtained using (*R*)-(−)-DBD-Py-NCS ($R_s = 3.45$). In addition, compared with using conventional HPLC, about 2 times faster enantioseparations of D2PM and MPH could be possible using UHPLC. Therefore, in this study, (*R*)-(−)-DBD-Py-NCS was used as the chiral derivatization reagent.

Rapid enantiomeric separation and determination of phenethylamines from the products distributed in the Japanese market by UHPLC–ESI-TOF-MS

Table 2 lists the retention time (t_R), *m/z*, α, and R_s for enantiomeric resolution of phenethylamines using (*R*)-(−)-DBD-Py-NCS as a chiral derivatization reagent. Enantiomeric separations of eight phenethylamines (BDB, D2PM, 4FMP, bk-MBDB, bk-MDEA, 4-methylmethocatinone, MPH, and PMMA) was achieved using H_2O–CH_3OH–FA (45:55:0.1, *v/v/v*) as the mobile phase. Also, DOI, *N*-ethylcatinone, *N*-methyl-FMP, and MMDA-2 were enantiomerically separated using H_2O–CH_3CN–FA (62:38:0.1, *v/v/v*) as the mobile phase.

The proposed method was applied to the determination of phenethylamine products obtained from an adult shop and via the Internet. The products were extracted with H_2O–CH_3OH, centrifuged, filtered, derivatized by (*R*)-(−)-DBD-Py-NCS, and then analyzed by UHPLC–ESI-TOF-MS. Typical chromatograms obtained from these products are shown in Figure 3. BDB and MMDA-2 were detected from products 1 and 2, respectively, and they were identified as racemic. High-resolution mass analysis by ESI-TOF-MS provided excellent accuracy in the determination of the *m/z* of the derivatives (less than 1.8 ppm). Since the products analyzed in this study contained simple racemic forms, it would be difficult to trace the manufacturing method or sources. However, in combination with impurity analysis of the products, the proposed method is expected to be applicable for such purposes.

Analysis of D2PM in rat hair by UHPLC-FL

Hair specimens are suitable for retrospective analyses when blood and urine are no longer expected to contain the illicit drugs.[30–34] Hair is typically suitable for this kind of analysis for several months up to one year after ingestion. In addition, once incorporated into hair, drugs are protected by a cuticle layer and are almost independent of daily cleaning. The developed method was also applied to the analysis of illicit drugs in hair specimens in which rats were administered oral doses (40 mg/kg day) of D2PM continuously for three weeks. The hair specimens were analyzed by FL, which has a wide dynamic rage and superior quantitative performance compared with ESI-TOF-MS.

Acidic methanol extraction was used for the analysis of D2PM-dosed rat hair specimens. CH_3OH–TFA (50:1, *v/v*) was used as an extraction solvent since D2PM was extracted efficiently, and TFA is volatile. When CH_3OH–5 M HCl (9:1, *v/v*) was used for extraction, HCl remained after removal of the solvent by nitrogen

gas. Therefore, the ratio of derivatization reaction decreased dramatically, and sufficient peak intensity of (*R*)-D2PM, (*S*)-D2PM, and PBH (internal standard) was not obtained (data not shown).

Figure 4A shows that no endogenous constituents of blank hair extracts eluted at the retention times of the peaks of (*R*)-D2PM, (*S*)-D2PM, or PBH. Adequate separation and detection were achieved within 7 min using H_2O–CH_3OH–FA (40:60: 0.1, *v/v/v*) as the mobile phase (Figures 4B–4F). Therefore, the developed method was found to be selective for (*R*)- and (*S*)-D2PM in hair specimens without interferences from normal endogenous hair constituents.

Calibration curves were obtained using blank hair spiked with (*R*)- and (*S*)-D2PM. The curves obtained by plotting the peak area ratios of (*R*)- and (*S*)-D2PM relative to the internal standard exhibited good linearity ($r^2 > 0.999$). The precisions of different concentrations (QCL and QCH) were also evaluated by intra- and inter-day assays. As shown in Table 3, the precision of the intra- and inter-day assays were 2.73–6.53% and 4.11–6.64%, respectively; thus, reasonable precisions were obtained. The detection limits of (*R*)- and (*S*)-D2PM were 0.12 ng/mg hair and 0.21 ng/mg hair, respectively (signal-to-noise ratio (S/N) = 3). Table 4 lists the amounts of (*R*)- and (*S*)-D2PM detected from rat hair. Although variability among individual rats was observed, (*R*)-form was detected from the rat dosed with (*R*)-form, (*S*)-form was detected from the rat dosed with (*S*)-form, and both (*R*)- and (*S*)-form were detected from the rat dosed with the racemic form, as expected.

Although conventional acidic methanol extraction requires long preparation times for hair specimens, by applying macropulverized extraction,[25,35] rapid enantiomeric separation and quantification of D2PM in hair was achieved. The proposed method should be useful for preventing widespread distribution of D2PM as a new illegal drug and is also expected to be appropriate for the analysis of human hair specimens from drug abusers.

Conclusion

In this study, rapid enantiomeric separation of phenethylamine-type abused drugs was accomplished using (*R*)-(−)-DBD-Py-NCS as the chiral fluorescent derivatization reagent based on UHPLC. Enantiomeric separation of 12 phenethylamines was achieved. The proposed method was successfully applied to the analysis of products containing illicit drugs distributed in the Japanese market. Among the products, BDB and MMDA-2 were detected in racemic form. The method was also applied to the analysis of rat hair specimens in which the rats were administered oral doses of D2PM. The proposed method should be useful for preventing widespread distribution of D2PM as a new illicit drug and is also expected to be applicable to the analysis of human hair specimens from drug abusers.

Acknowledgements

This work was supported in part by a health sciences research grant from the Ministry of Health Labour and Welfare, and a research grant from the Ministry of Education, Culture, Sports, Science and Technology, Japan.

References

[1] N. Uchiyama, N. Miyazawa, M. Kawamura, R. Kikura-Hanajiri, Y. Goda. Analysis of newly distributed designer drugs detected in the products purchased in fiscal year 2008. *Yakugaku Zasshi* **2010**, *130*, 263.
[2] K. Doi, M. Miyazawa, H. Fujii, T. Kojima. The analysis of the chemical drugs among structural isomer. *Yakugaku Zasshi* **2006**, *126*, 815.
[3] D.M. Wood, J. Buttun, S. Lidder, H. Ovska, J. Ramsey, D.W. Holt, *et al.* Detection of the novel recreational drug diphenyl-2-pyrrolidinemethanol (D2PM) sold 'legally' in combination with glaucine. *Clin. Toxicol.* **2008**, *46*, 393.
[4] S. Lidder, P.I. Dargan, M. Sexton, J. Button, J. Ramsey, D.W. Holt, *et al.* Cardiovascular toxicity associated with recreational use of diphenylprolinol (diphenyl-2-pyrrolidinemethanol [D2PM]). *J. Med. Toxicol.* **2008**, *4*, 167.
[5] D. Enders, M.R.M. Hüttl, C. Grondal, G. Raabe. Control of four stereocentres in a triple cascade organocatalytic reaction. *Nature* **2006**, *441*, 861.
[6] B.B. Lohray, V. Bhushan. Oxazaborolidines and dioxaborolidines in enantioselective catalysis. *Angew. Chem. Int. Edit. Engl.* **1992**, *31*, 729.
[7] E.J. Corey, R.K. Bakshi, S. Shibata. Highly enantioselective borane reduction of ketones catalyzed by chiral oxazaborolidines – mechanism and synthetic implications. *J. Am. Chem. Soc.* **1987**, *109*, 5551.
[8] M.R. Meyer, H.H. Maurer. Metabolism of designer drugs of abuse: An updated review. *Curr. Drug Metabolism* **2010**, *11*, 468.
[9] National Highway Traffic Safety Administration (NHTSA). Drugs and human performance fact sheets. *Methamphetamine and Amphetamine*. NHTSA, Washington, DC, **2004**, pp. 61–65.
[10] C. Borst, U. Holzgrabe. Comparison of chiral electrophoretic separation methods for phenethylamines and application on impurity analysis. *J. Pharm. Biomed. Anal.* **2010**, *53*, 1201.
[11] T.J. Ward, K.D. Ward. Chiral separations: Fundamental review 2010. *Anal. Chem.* **2010**, *82*, 4712.
[12] T. Ikai, Y. Okamoto. Structure control of polysaccharide derivatives for efficient separation of enantiomers by chromatography. *Chem. Rev.* **2009**, *109*, 6077.
[13] B. Preinerstorfer, M. Laemmerhofer, W. Lindner. Advances in enantioselective separations using electromigration capillary techniques. *Electrophoresis* **2009**, *30*, 100.
[14] A. Ghassempour, H.Y. Aboul-Enein. Vancomycin degradation products as potential chiral selectors in enantiomeric separation of racemic compounds. *J. Chromatogr. A* **2008**, *1191*, 182.
[15] T.E. Beesley, R.P.W. Scott. *Chiral Chromatography*. John Wiley & Sons Ltd, New York, USA, **1999**.
[16] S. Ahuja. *Chiral Separation Methods for Pharmaceutical and Biotechnological Products*. John Wiley & Sons Ltd, New York, USA, **2010**.
[17] V. Cucinotta, A. Contino, A. Giuffrida, G. Maccarrone, M. Messina. Application of charged single isomer derivatives of cyclodextrins in capillary electrophoresis for chiral analysis. *J. Chromatogr. A* **2010**, *1217*, 953.
[18] V. Pérez-Fernández, M.Á. García, M.L. Marina. Characteristics and enantiomeric analysis of chiral pyrethroids. *J. Chromatogr. A* **2010**, *1217*, 968.
[19] D. Guillarme, G. Bonvin, F. Badoud, J. Schappler, S. Rudaz, J.-L. Veuthey. Fast chiral separation of drugs using columns packed with sub-2 μm particles and ultra-high pressure. *Chirality* **2010**, *22*, 320.
[20] S. Inagaki, S. Taniguchi, H. Hirashima, T. Higashi, J.Z. Min, R. Kikura-Hanajiri, *et al.* HPLC enantioseparation of α,α-diphenyl-2-pyrrolidinemethanol and methylphenidate using a chiral fluorescent derivatization reagent and its application to the analysis of rat plasma. *J. Sep. Sci.* **2010**, *33*, 3137.
[21] D. Guillarme, J. Ruta, S. Rudaz, J.-L. Veuthey. New trends in fast and high-resolution liquid chromatography: a critical comparison of existing approaches. *Anal. Bioanal. Chem.* **2010**, *397*, 1069.
[22] T. Toyo'oka. Determination methods for biologically active compounds by ultra-performance liquid chromatography coupled with mass spectrometry: Application to the analyses of pharmaceuticals, foods, plants, environments, metabonomics, and metabolomics. *J. Chromatogr. Sci.* **2008**, *46*, 233.
[23] R.N. Xu, L. Fan, M.J. Rieser, T.A. El-Shourbagy. Recent advances in high-throughput quantitative bioanalysis by LC–MS/MS. *J. Pharm. Biomed. Anal.* **2007**, *44*, 342.
[24] S. Lee, H. Miyaguchi, E. Han, E. Kim, Y. Park, H. Choi, *et al.* Homogeneity and stability of a candidate certified reference material for the determination of methamphetamine and amphetamine in hair. *J. Pharm. Biomed. Anal.* **2010**, *53*, 1037.

[25] H. Miyaguchi, M. Kakuta, Y.T. Iwata, H. Matsuda, H. Tazawa, H. Kimura, *et al.* Development of a micropulverized extraction method for rapid toxicological analysis of methamphetamine in hair. *J. Chromatogr. A* **2007**, *1163*, 43.
[26] M.J. Welch, L.T. Sniegoski, S. Tai. Two new standard reference materials for the determination of drugs of abuse in human hair. *Anal. Bioanal. Chem.* **2003**, *376*, 1205.
[27] T. Toyo'oka. Fluorescent chiral derivatization reagents possessing benzofurazan structure for the resolution of optical isomers in HPLC: The synthesis, characteristics and application. *Curr. Pharm. Anal.* **2005**, *1*, 57.
[28] T. Toyo'oka, Y.-M. Liu. Development of optically active fluorescent Edman-type reagents. *Analyst* **1995**, *120*, 385.
[29] T. Toyo'oka, Y.-M. Liu. High-performance liquid chromatographic resolution of amino acid enantiomers derivatized with fluorescent chiral Edman reagents. *J. Chromatogr. A* **1995**, *689*, 23.
[30] P. Kintz. Bioanalytical procedures for detection of chemical agents in hair in the case of drug-facilitated crimes. *Anal. Bioanal. Chem.* **2007**, *388*, 1467.
[31] F. Musshoff, B. Madea. New trends in hair analysis and scientific demands on validation and technical notes. *Forensic Sci. Int.* **2007**, *165*, 204.
[32] V.A. Boumba, K.S. Ziavrou, T. Vougiouklalis. Hair as a biological indicator of drug use, drug abuse or chronic exposure to environmental toxicants. *Int. J. Toxicol.* **2006**, *25*, 143.
[33] P. Kintz, M. Villain, V. Cirimele. Hair analysis for drug detection. *Ther. Drug Monit.* **2006**, *28*, 442.
[34] K. Srogi. Testing for drugs in hair-a review of chromatographic procedures. *Microchim. Acta* **2006**, *154*, 191.
[35] S. Inagaki, H. Makino, T. Fukushima, J.Z. Min, T. Toyo'oka. Rapid detection of ketamine and norketamine in rat hair using micropulverized extraction and ultra-performance liquid chromatography–electrospray ionization mass spectrometry. *Biomed. Chromatogr.* **2009**, *23*, 1245.

Research article Chromatography

Received 4 January 2011, Accepted 19 January 2011 Published online in Wiley Online Library: 9 March 2011

(wileyonlinelibrary.com) DOI 10.1002/bmc.1619

Simultaneous determination of *N*-benzylpiperazine and 1-(3-trifluoromethylphenyl)piperazine in rat plasma by HPLC-fluorescence detection and its application to monitoring of these drugs

Mitsuhiro Wada[a], Kozue Yamahara[a], Rie Ikeda[a], Ruri Kikura-Hanajiri[b], Naotaka Kuroda[a] and Kenichiro Nakashima[a]*

ABSTRACT: An HPLC-fluorescence detection method for simultaneous determination of *N*-benzylpiperazine (BZP) and 1-(3-trifluoromethylphenyl)piperazine (TFMPP) labeled with 4-(4,5-diphenyl-1 *H*-imidazol-2-yl)benzoyl chloride (DIB-Cl) was described. DIB-BZP and -TFMPP were well separated within 13 min without interference of peaks from plasma components. The lower detection limits of BZP and TFMPP at a signal-to-noise ratio of 3 were 0.9 and 4.6 ng/mL, respectively. Precisions of the proposed method for intra- and inter-day assays were less than 4.8 and 9.1% as %RSD ($n = 5$). Furthermore, the method could be successfully applied to monitor both compounds in plasma after their sole or co-administration to rats (each dose, 2 mg/kg). Clearance of TFMPP was significantly different under the conditions ($P = 0.047$). Copyright © 2011 John Wiley & Sons, Ltd.

Keywords: benzylpiperazine (BZP); 1-(3-trifluoromethylphenyl)piperazine (TFMPP); DIB-Cl; HPLC-fluorescence detection; rat plasma

Introduction

The drugs of abuse 'piperazines' comprise two classes: benzylpiperazines such as *N*-benzylpiperazine (BZP) and phenylpiperazines, 1-(3-trifluoromethylphenyl)piperazine (TFMPP). Drug abusers have reportedly ingested BZP and/or TFMPP in an attempt to mimic the 3,4-methylenedioxymethamphetamine (MDMA) subjective experience (de Boer *et al.*, 2001; Butler and Sheridan 2007; Fantagrossi *et al.*, 2005). Evidence of the effects of piperazines from neurochemical (Baumann *et al.*, 2004, 2005) and behavioral pharmacological (Yarosh *et al.*, 2007) viewpoints has been reported. Adverse reactions such as dissociative, sympathomimetic symptoms associated with recreational use of BZP and/or TFMPP have also been reported (Wood *et al.*, 2008; Austin and Monasterio 2004).

'Party pills' containing both BZP and TFMPP have been seized worldwide (Wood *et al.*, 2007; Cuddy, 2004; Wilkins and Sweetsur 2010), and have caused serious social problems. In particular, a big market for party pills containing piperazines existed in New Zealand from the early 2000s until their prohibition in 2008 (Wilkins and Sweetsur, 2010). To date, the pharmacokinetics of piperazines and their drug interactions have been extensively studied, although they have not been completely clarified (Antia *et al.*, 2009a, 2009b). A simultaneous determination method for BZP and TFMPP might be useful to clarify the interactions in detail and will help in the prediction of and the protection of human health against the risks of piperazines.

Several analytical methods have been reported for the determination of BZP and/or TFMPP. Among these, gas chromatography–mass spectrometry (GC-MS; Staack *et al.*, 2002; Staack and Maurer, 2003; Vorce *et al.*, 2008; Peters *et al.*, 2003; Tsutsumi *et al.*, 2005a, 2005b, 2006), HPLC-UV (Elliott and Smith, 2008), liquid chromatography (LC)-MS (Antia *et al.*, 2009a; Vorce *et al.*, 2008; Tsutsumi *et al.*, 2005b, 2006; Elliott and Smith, 2008) and capillary electrophoresis–UV (Bishop *et al.*, 2005) methods were examined. However, UV detection was not sensitive enough to determine these compounds in biological matrices. MS detection, having high sensitivity and selectivity, could achieve low-level quantification of piperazines in biological samples within a short analytical time, although a MS detector is an expensive piece of equipment with tedious maintenance and is not in ordinary, widespread use.

Fluorescence (FL) labeling is a powerful tool to determine compounds having no desirable properties in their structure for sensitive spectrophotometric determination, and has been used to determine trace amounts of biologically active compounds

* Correspondence to: K. Nakashima, Department of Clinical Pharmacy, Graduate School of Biomedical Sciences, Nagasaki University, 1-14 Bunkyo-machi, Nagasaki 852-8521, Japan. E-mail: naka-ken@nagasaki-u.ac.jp

[a] Department of Clinical Pharmacy, Graduate School of Biomedical Sciences, Nagasaki University, 1-14 Bunkyo-machi, Nagasaki 852-8521, Japan

[b] National Institute of Health Sciences, 1-18-1 Kamiyoga, Setagaya, Tokyo 158-8501, Japan

Abbreviations used: BZP, *N*-benzylpiperazine; DIB-Cl, 4-(4,5-Diphenyl-1 *H*-imidazol-2-yl)benzoyl chloride; FL, fluorescence; FLI, FL intensities; TFMPP, 1-(3-trifluoromethylphenyl)piperazine.

such as drugs in biological samples (Nakashima *et al.*, 2009). 4-(4,5-Diphenyl-1 *H*-imidazol-2-yl)benzoyl chloride (DIB-Cl), a fluorescence labeling reagent synthesized by us, reacts with compounds that have amino and hydroxyl groups to produce intense fluorogenic labels (Nakashima *et al.*, 2009). In our previous studies, highly sensitive and selective determination of drugs of abuse such as amphetamine analogs (Nakamura *et al.*, 2007; Kaddoumi *et al.*, 2004) and narcotics (Wada *et al.*, 2007, 2008) has been achieved. Thus we consider that sensitive determination of piperazines such as BZP and TFMPP might be achieved by an HPLC-FL method combined with DIB-labeling, although no HPLC-FL method with labeling has ever been reported.

In this study an HPLC-FL detection method for simultaneous determination of BZP and TFMPP labeled with DIB-Cl was developed. Furthermore, the proposed method was applied to monitor both compounds in plasma after a single sole or co-administration to rats.

Materials and methods

Chemicals

BZP was a gift from the Narcotics Control Department, Kanto-Shin'etsu Bureau of Health and Welfare (Tokyo, Japan). TFMPP was kindly given by the National Institute of Health Sciences (Tokyo, Japan). DIB-Cl was obtained from Tokyo Kasei Kogyo Co. (Tokyo, Japan). Other reagents used were of analytical grade. Water was purified by a Pure Line WL21P system (Yamato Scientific Co., Tokyo, Japan). Stock standard solutions (1 mg/mL) of BZP and TFMPP were prepared by dissolving in CH_3CN and stored at −30°C until analysis.

Instruments

The HPLC system for separation of DIB-BZP and -TFMPP labels consisted of two chromatographic pumps (LC-10AD$_{VP}$, Shimadzu, Kyoto, Japan), a system controller (SCL-10 AD$_{VP}$, Shimadzu), a 7125 injector with a 20 µL sample loop (Rheodyne, CA, USA), a Daisopak-SP-ODS-BP column (250 × 4.6 mm, i.d., 5 µm, Daiso, Osaka, Japan), a column oven (CTO-6AS, Shimadzu), an RF10A$_{XL}$ fluorescence detector (Shimadzu) and a recorder (R-01A, Rikadenki, Tokyo, Japan). The solutions of 0.1 M acetate buffer (pH 3.5, MP 1) and CH_3CN (MP 2) were used as mobile phases and the total flow rate was set at 1.0 mL/min. The gradient program to separate DIB labels was set as follows: the ratio of MP 2 was initialized at 63% (0–4.0 min), linearly ramped to 80% (4.1–7.0 min), kept at 80% (7.1–8.0 min), then linearly ramped to 70% (8.1–11.0 min), kept at 70% (11.1–14.0 min), changed to 95% (14.1–19.0 min) for washing and then reduced to 63% (19.1–24.0 min) for equilibration of the analytical column. Column temperature was set at 35°C, and eluates were monitored at 340 nm (λ_{ex}) and 445 nm (λ_{em}).

Pretreatment of plasma sample

To 20 µL of plasma, 50 µL each of 0.1 M carbonate buffer (pH 9.0) and 0.2 mM DIB-Cl in CH_3CN suspension were added. The reaction mixture was stood at room temperature for 30 min, and then 10 µL of 25% NH_3 aqueous solution was added to stop the labeling reaction.

The resultant mixture was cleaned up by a SPE cartridge to eliminate excess reagent and interfering materials for detection of DIB-BZP and -TFMPP. A 130 µL aliquot of labeled mixture were applied to Varian Bond Elut® C_{18} (Varian Technologies Japan Ltd, Tokyo, Japan) which was conditioned with H_2O and CH_3CN before use. The cartridge was washed triplicate with 1 mL of CH_3CN/H_2O (40:60, v/v). Then the DIB labels were eluted with 500 µL of CH_3CN. The eluate was dried up under N_2 gas and the residue was reconstituted with 100 µL of CH_3CN for HPLC analysis.

Method validation

For determination of BZP and TFMPP, calibration curves using rat plasma spiked with known concentration of standards were prepared. Spiked plasma samples in the ranges of 25–1000 ng/mL for BZP and of 50–2000 ng/mL were prepared. The limits of detection (LOD) and quantification (LOQ) were defined as the concentration giving signal-to-noise (S/N) ratios of 3 and 10, respectively. Recovery of the proposed method was expressed as the peak height ratio of standards spiked in plasma with SPE clean-up on standards without clean-up. Accuracy and precision for inter-day and intra-day assay were evaluated using plasma samples spiked with 50 and 500 ng/mL of BZP, and 100 and 1000 ng/mL of TFMPP, respectively. Data was expressed as mean ± SD ($n = 5$).

Monitoring of BZP and TFMPP after their sole or co-administration to rats

Wistar male rats (280–300 g, Otsubo Experimental Animals, Nagasaki, Japan) were used. Rats were anesthetized with ethyl carbamate (1.5 g/kg, i.p.) before cannulation. From the cannulated femoral artery, blood samples were collected into the test tube containing EDTA-2Na for preparation of plasma. Blood sampling was performed at 0, 15, 30, 45, 60, 90, 120, 180, 240, 300 and 360 min after sole or co-administration of the compounds (2 mg/kg, i.p.). After centrifugation (1000 *g*) at 4°C for 10 min, plasma was kept at −30°C until analysis. The pharmacokinetic parameters such as elimination rate constant (K), elimination half-life ($T_{1/2}$), distribution volume (V) and clearance (Cl) of the compounds were calculated using a one-compartment model analysis. The area under the curve (AUC_{0-360}) of the compounds was calculated by a trapezoidal method. Statistical analysis was performed using an unpaired Student's *t*-test. Probability values less than 0.05 were considered significant. This experiment was performed with an approval of the Nagasaki University Animal Care and Use Committee.

Results and discussion

Pretreatment of samples

Labeling conditions such as DIB-Cl concentration, borate buffer pH, reaction time and temperature were optimized. By using 50 ng/mL of BZP and 100 ng/mL of TFMPP standard solutions, FL intensities (FLI) of their DIB labels were measured for evaluation. The effects of DIB-Cl concentration (0.01–1.0 mM) on the FLI were examined, and it was found that DIB labels gave the maximum and constant FLI with more than 0.05 mM. Thus the following experiments were done using 0.2 mM of DIB-Cl. Borate buffer pH ranging from 8.5 to 11.0 was examined, and the maximum FLI of both compounds was achieved at pH 9.0. Effects of reaction time at room temperature and 60°C on FLI of labels were studied, and the maximum FLI was obtained with more than 30 min of reaction

